A comparison of modelling approaches for the evaluation of the electrical performance of secondary batteries in battery management systems (BMS)

Mirko D'Adamo

Thesis to obtain the Master of Science Degree in

Energy Engineering and Management

Supervisors: Prof. Luísa Margarida Dias Ribeiro de Sousa Martins
Prof. Francisco Díaz-González

Examination Committee

Chairperson: Prof. Francisco Manuel de Silva Lemos
Supervisor: Prof. Francisco Díaz-González
Member of the Committee: Prof. Sónia Maria Nunes dos Santos Paulo Ferreira Pinto

October 2021

To whoever has been affected by this Crisis
may you find the strength to bounce back,
you have much more than you think
to share with this world

Acknowledgments

I would like to thank my family who gave me the opportunity to embark on this journey. The University of Lisbon, IST to make me experience and learn so much.

I want to special thank my Professor and supervisor, Francisco Diaz-Gonzalez to make me passionate about the world of Battery and Battery modeling. Without you as professor, I would not have even started this thesis .

I would like to thank my Supervisor Luísa Margarida Martins that has been open to my Thesis Idea and to understand my moments of difficulties that this Crisis generated.

Finally, I would like to thank whoever I have come across along this Master journey. You helped me to grow and strengthen my self-consciousness. Because, more than the subjects and the degree itself, what really matters in this experience is the network you create. Knowledge must be shared!

Resumo

Os valores dos sistemas de gestão de baterias (BMS) nas baterias dos veículos híbridos elétricos (HEV) têm de se aproximar de valores que descrevam o estado operacional atual da bateria. São exemplos destes sistemas o estado de carga de uma bateria (SOC) e a potência instantânea disponível. O processo de estimativa tem de ser capaz de responder a variações nas características das células das baterias, à medida que estas envelhecem, de modo a produzir previsões confiáveis ao longo do seu ciclo de vida. Um sistema baseado no filtro de Kalman estendido (EKF) pode atingir estes objetivos numa bateria de ião lítio com química de NMC/grafite. Esta dissertação aborda vários modelos matemáticos de células que podem ser usados para a referida abordagem. A implementação de HEV constitui um ambiente drástico, com especificações de velocidade até, e superiores a, 20 graus Celsius e perfis de velocidade complexos. Em comparação, os aparelhos eletrónicos portáteis, com um potencia de saída constante, e velocidades C fracionais são relativamente benignos. Os métodos de cálculo de SOC adequados para os aparelhos eletrónicos portáteis, não o são para os HEV. Se um HEV necessitar de uma estimativa precisa de SOC, será necessário um modelo extremamente preciso. Quando o input da célula modelo é igual à corrente da célula, o objetivo é conseguir que o output da célula modelo seja sempre o mais aproximado possível da voltagem terminal da célula sob carga. Nesta dissertação foram implementados três modelos diferentes para estimar a voltagem terminal da célula, em ambiente MATLAB/Simulink. Estes três modelos matemáticos foram implementados adicionalmente num quarto modelo elétrico designado Modelo de Thevenin. São apresentados os resultados para demonstrar a estimativa final de voltagem como próxima da voltagem real e a estimativa de SOC para os todos os modelos de célula propostos.

Palavras-chave: sistemas-de-gestão-de-baterias (BMS), estado-de-carga (SOC), The-combined-model,The-simple-model, The-zero-state hysteresis-model, The-thevenin-model.

Abstract

In hybrid electric vehicle battery packs, battery management systems (BMS) must approximate values that describe the pack's current operating state. Battery state of charge(SOC) and instantaneous usable power are examples of these. The estimation process must respond to changing cell characteristics as cells age in order to produce reliable predictions over the pack's lifespan. To suggest a system based on extended Kalman filtering(EKF) that can achieve these objectives on a lithium-ion battery pack with NMC/graphite chemistry. This report discusses several mathematical cell models that can be used in connection with this approach. The HEV implementation is a harsh environment, with rate specifications up to and above 20 degrees Celsius and very complex rate profiles. In comparison, portable-electronic devices with steady power output and fractional C rates are relatively benign. Methods for calculating SOC that work well in portable electronics cannot work well in HEVs. If the HEV requires precise SOC estimation, then highly accurate cell model is needed. When the cell model input is equal to the cell current, the target is to make the cell model output resemble the cell terminal voltage under load as near as possible at all times. In this research report, three different models for cell to estimate terminal voltage have been implemented in MATLAB/Simulink environment. The three mathematical models are further implemented in a fourth electrical model called Thevenin Model. Results are presented to demonstrate the terminal estimation voltage as close to actual voltage and SOC estimation for all the proposed cell models.

Keywords: Battery management system (BMS), State of charge (SOC), The combined model, simple model, The zero-state hysteresis model, The thevenin model

Contents

List of Tables

List of Figures

GLOSSARY

BEV=Battery Electric Vehicle

BMS= Battery Management Systems

BNEF= Bloomberg New Energy Finance

CALCE=Center forAdvanced Life Cycle Engineering

CMU= Cell Monitoring unit

CSC= Cell Supervision Circuits

EV= Electric Vehicle

GHG= Greenhouse Gases

GWh= Gigawatt hour

HEV= Hybrid Electric Vehicle

ICE = Internal Combustion Engine

kWh=Kilowatt hour

LiPF6 = Lithium hexafluorophosphate

LMO= Lithium Manganese spinel

MMU = Module Monitoring Unit

NMC= Lithium-ion Nichel Manganese Cobalt Oxide

NMA= Nickel Manganese and aluminum

OCV= Open Circuit Voltage

PMU=Pack Management Unit PMU

SOC = State of charge

Chapter 1

Preface

The aim of the following thesis is to explore different lithium-ion battery modelings with the objective to find the best estimation of its State-of-Charge. This parameter is paramount for the calculation then, of other parameters such as Energy availability, Power availability in a specific time window and Life of the battery. An optimal Algorithm coupled with a Battery Management Systems can make the difference in terms of cost, environmental impact, life of the battery, user interface and battery performances depending on the type of technology using this battery as power source. Moreover, further issues are about which methods give the best battery parameters estimation .

This thesis will analyse literature about lithium-ion battery modelings and four of them will be utilized to find the best parameter estimation. The author will so make a comparison among of them try to understand the best solutions according to the context where such Data Algorithms can be implemented.

To conclude this thesis, the environmental impact of the rising Electromobility demand on lithium and the lithium-ion battery market will be explored.

1.1 Motivation of the project

The main motivation to the project is my personal concern about how climate change will have an impact on my present and future life. According to the last trend, energy transition is the only chance to make the planet Earth a better place to live in. The rapid growing demand of electromobility and the opportunity to integrate renewable energy to the grid ask for a quick improvement in terms of energy storage.

Lithium-ion battery are the battery most used nowadays and need still a plethora of further exploitation in order to extend their life and to have a carbon foot-print equal to zero. My personal concern is to try to give a positive contribute in better understanding the main challenges that need still to be aggressively tackled to achieve a positive impact on the global decarbonization.To sum up, this thesis try to further understand the impact of the fast growing demand of energy storage on Lithium sources.

Chapter 2

Introduction

Nowadays, we are witnessing a global issue related to the increase of GHG emissions and the devastating impact they have on the present and the future life on this planet. Governments and public organizations are tackling this problem by pushing research to develop new technologies to help the energy transition, assuring us to go from fossil fuel dependency to a greener one. An important trend to mention that is actually disrupting the new market transportation is the world electrification. There is a rapid growing demand in the electromobility industry that asks for high energy storage capability [1].Moreover, portable devices are rising in demand rapidly as well.

The most used and well performing technology in this sector is Lithium-ion battery. Having a still high cost but forecasted to be constantly dropping over the next decade, there is a need to extend their life and improve their performances. Currently, this technology is monitored from an embedded system called Battery Management System which assures the safety of the battery by constantly monitoring the battery and communicating with the user. However, It is not quite easy to calculate Power and Energy availability. To do so, there are several methods that go from chemistry based ones to data algorithms that must be run by the BMS. One of the parameters that cannot be easily measured when the user is using the battery is the State-of-charge (Soc). There are several models which predict/estimate this parameter which is crucial to further calculate the power availability, energy availability and the remaining life of the battery. This is the biggest challenge this report wants to address.

2.1 Challenge faced

The hybrid electric vehicle (HEV) implementation is a harsh environment, with rate specifications up to and above 20 degrees Celsius and very complex rate profiles. In comparison, portable-electronic devices with steady power output and fractional C rates are relatively benign. Methods for calculating SOC that work well in portable electronics can not work well in HEVs. If the HEV requires precise SOC estimation, then a highly accurate cell model is needed. Several direct SOC calculation approaches are clearly not applicable in present application:

A laboratory approach for measuring SOC is to discharge a cell entirely and record the discharged ampere-hours to calculate the cell's current remaining energy. This is the most precise SOC estimation technique, but it is inefficient in HEVs since the test wastes battery resources and can't dynamically estimate SOC. Other chemistry-dependent techniques, such as Coup de Fouet measurement or electrolyte physical property measurement for lead-acid batteries, are all ineffective. When a cell is forced to rest for a long time, its terminal voltage decays to Open Circuit Voltage (OCV), which can be used to infer SOC (for example, using a lookup table). Long periods of battery inactivity (sometimes hours) are needed before the terminal voltage reaches OCV. This approach should not be used to estimate complex SOC. Other drawbacks of this approach include OCV's temperature dependence and the presence of terminal voltage hysteresis, especially at low temperatures.

2.2 Work development and objectives

Advanced algorithms for a BMS for hybrid electric vehicle (HEV) applications are defined in this report. This BMS calculates SOC and instantaneous power available to the battery. It also adjusts to changing cell characteristics as the battery pack ages. . The algorithms were tested on a lithium-ion with nickel-manganese-cobalt-oxide(NMC) cathode and graphite anode battery pack previously tested at Center for Advanced Life Cycle Engineering (CALCE), University of Maryland [2], but they should work for other battery chemistries as well.In particular, the author carried out a Traineeship at University Politecnica de Catalunya. The approach he uses to approximate these parameters is based on the theory of the Kalman filter. Other methods for SOC estimation that use Kalman filtering have been published [3, 4], but the approach here builds on these findings while still differing in certain important ways. Kalman filters are intelligent and often optimal method of estimating the state of a complex system. By modelling our battery scheme so that the desired unknown quantities are included in the "state," we can use the Kalman filter to approximate their values. Another advantage of using the Kalman filter is that it automatically gives complex error-bounds on these predictions which has not developed in this report.The three mathematical models used in this project are further implemented in a Fourth electrical model called Thevenin Model.

The outcomes of laboratory experiments on physical cells are interpreted and compared to model predictions.More specifically, the model provides for extremely accurate SOC prediction, enabling the vehicle controller to safely use the battery pack's maximum operating range without fear of over- or under-charging batteries.

2.3 Thesis Outline

The author dedicated the chapter 3 of this work to literature review where he explained the functionality and architecture of Battery Management System followed by a list of the most used Models to estimate the Soc of Lithium-ion battery. Sub-sequentially, he addressed the chapter 4 four to the Methodology used: Block diagram of the tools adopted and developed to face the problem. After that he showed the development of the different phases of the methodology .

The chapter 5 has been used to introduce the study case where the author worked on, describing the inputs data and execute tools adopted in the previous section. In this chapter, the author also showed the results obtained analyzing the plots generated by the several models used.

In the following chapter 6 the author discussed the results obtained. The chapter 7talks about the Environmental Impact of this project. In the chapter 8, the author talked about the cost of the project and shows the lithium-ion battery market. Afterwards, conclusions have been made by the author.

Chapter 3

Background

Lithium -ion battery is the technology that gives the best performances among the electrochemical batteries in Electromobility sector. The performances are more and more demanding: users ask for the possibility to run long trip, to have a fast charge and high-power capability to guarantee high performance of the vehicle. These types of batteries had a big success also due to their high energy and power density which means the chance to have a remarkable energy and power availability keeping the weight parameter still low.

On the other hand, even though this technology has shown considerable advantages, it has done so also for the drawbacks: Lithium -ion battery is not safe in every working condition [5]. For instance, because of the electrochemistry temperatures needs to be constantly monitored where overcoming some limits such as temperature, voltage and current the battery can be affected by an exothermic reaction called thermal runway which is irreversible and can lead to set on fire the battery pack.

Regarding the most frequent problematic conditions, it can be found: over-voltage, deep discharge and over current. Moreover, there has been the need to communicate to the user the presence of safety problems, the current energy and or power available and state of health of the battery.

These challenges have been being addressed by new architectures which are progressively increasing their reliability, allowing to save much money: Battery Management Systems. Nowadays, as described in the section before Battery in Electromobility sector makes widely use of a physical architecture called BMS which stands for Battery Management Systems.

The use of this tool has been largely discussed.

3.1 Battery Management Systems

Definition of BMS:

The BMS is an analogue or digital electronic device managing and electronic safety circuitry [6] to perform specific functions that can change according to its use. It is an embedded system(purpose-built electronics plus processing to enable a specific application)[7]. Generally, must perform the following requirements: Data acquisition, Data processing and data storage, Electrical management, Temperature management, Safety management, and Communication.

3.2 BMS functionality

Why do we need a BMS? The BMS must operates the following priorities [7]:

- Protects the safety of the battery operated device's operator
- Detects unsafe operating conditions and responds.
- Protects cells of battery from damage in abuse/failure cases.
- Prolongs life of battery (normal operating cases).
- Maintains battery in a state in which it can fulfill its functional design requirements.
- Informs the application controller how to make the best use of the pack right now (e.g., power limits), control charger, etc.

The BMS is associated to a battery pack. The BMS involves a big impact in terms of cost when we talk about large battery Pack such as Vehicular Application[7]. How do we understand if is necessary to invest in BMS rather than battery itself? The battery has still a huge cost even though is dropping constantly . However, the point to address is the use/application we are considering. For instance, in EV car is important to place a big investment in the BMS because this can help the user to prevent dysfunctions and prolong the life's battery itself. Another important aspect is that a good BMS can decrease the investment in Battery reducing the size needed. The BMS can be divided in five areas, each one fulfils

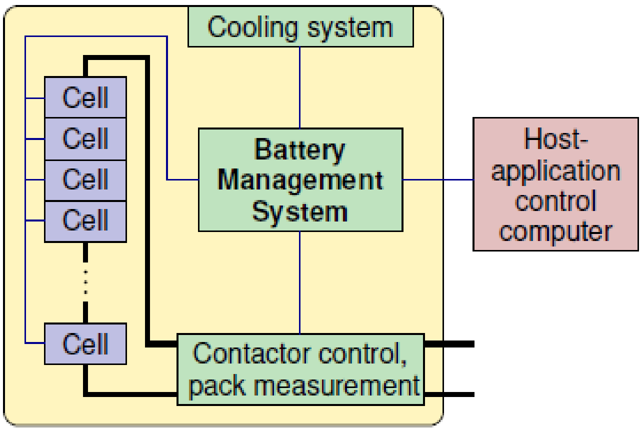

Figure 3.1: Bms functionalities [7]

different function: Sensing and high-voltage control, protection, Interfacing, Performance Management, diagnostics [7].

1. Sensing and high-voltage control: The BMS must measure cell voltages, module temperatures, and battery-pack current. It must also detect isolation faults and control the contactors and the thermal-management system.

2. Protection: The BMS must include electronics and logic to protect the operator of the battery-powered system and the battery pack itself against over-charge, over-discharge, over-current, cell short circuits, and extreme temperatures.

3. Interfacing: The BMS must communicate regularly with the application that the battery pack powers, reporting available energy and power and other indicators of battery-pack status. Further, it must record unusual error or abuse events in permanent memory for technician diagnostics via occasional on-demand download.

4. Performance management: The BMS estimates state-of-charge (SOC) for all the cells of the battery pack, compute battery-pack available energy and power limits, and balance (equalize) cells in the battery pack.

5. Diagnostics: Here the BMS estimates the remaining useful lifetime of the battery cells and pack.by calculating the state-of-health (SOH), showing possible overuses.

Bms architecture (components and topologies)

The bms can have different configurations, design and architecture. It is possible to identifies three subcomponents [8, 9] described from the lowest to Highest level:
Cell Monitoring unit (CMU): Every unit is linked to each cell providing their balancing while measuring their voltage, temperature and additional parameters.
Module Monitoring unit (MMU): Assures inter-cell balancing function managing a group o CMUs, (8÷12 cells) Pack management unit (PMU): Communicates with external systems and manage MMUs measuring parameters such as pack current and voltage.

Centralized BMS

Centralized Bms are the easiest pack where the three subcomponents are packed in only one, linking CMUs to MMus to PMU. Due to this layout it is difficult to scale it up. Indeed, it is more designed for battery with few number of cells like the case of electrical bicycles. Increasing the numbers of cells would affect the safety due to their wiring, getting complex.

Modular and Master-Slave BMS

In the Modular BMS instead, the problem with wiring is solved, leading to a less complex layout where PMU are linked to CMUs only indirectly and with MMUS through an interface.
On the other hand, Master-Slave Bms, is an advanced version of the modular, where it can be observed a reduction to a minimum and functions of the cell supervision circuits (CSC), implementing them only

on the master. [6].Slaves handle voltage/temperature measurements, balancing cell. Master handles current/Isolation sending, contactor control, thermal-management[7].

Distributed BMS

In a distributed BMS topology, every PMUs monitor their own set of cells or supercells, indeed they work autonomously, and they can easily communicate with other PMUs showing eventual fault.This kind of architecture is very flexible and scalable. On the other hand, it presents a high cost.

3.3 Battery estimation Soc Methods

As it has been shown before, SOC is one of the parameters that must be estimated by the Performance management of the BMS. It is not possible to measure how much energy or power is available. Instead, there are other parameters that must be calculated such as all well states-of-charges z_k, and capacities Q_k. For Power estimation must be estimated resistances R_k and all cell state-of-charge z_k.

However, at the same time these are values that cannot be directly measured so to estimate them, other inputs are needed. The above inputs are pack current, cell voltages, and temperatures of cells or modules. So, in order to compute the available energy and power BMS must estimate Soc as input.

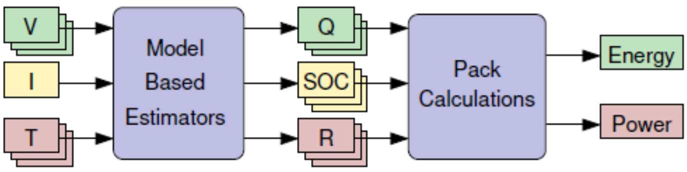

Figure 3.2: Soc flowchart[7]

State-of-charge

During charging and discharging cell moves lithium between negative and positive electrodes. Cell SOC related to average Li concentration in the negative-electrode particles.Voltage is useful as an indirect indicator of SOC, but not as measurement of SOC.The Cell voltage depends on Li surface concentration in particles that contact positive and negative current collectors. However, SOC depends on average concentrations over the entire electrode.The average concentrations are not affected by changing temperature, which changes voltage.Resting a cell, which changes voltage: does not change SOC. SOC changes only due to passage of current, either charging or discharging the cell due to external circuitry, or due to self-discharge within the cell [9].

$$z(t) = z(0) - \frac{1}{Q}\int_0^t \eta_i \, i\,(\tau)\; d\tau \tag{3.1}$$

This capacity Q is a physical quantity that measures the number of vacancies in the electrode structure and that crystal structure that could hold lithium between the stoichiometry of 0% and 100%. So this is not a function of temperature or rate. It is different from a discharge capacity which is what is commonly put on a data sheet for a battery cell. It's a total capacity, it's the total charge capacity.This equation is not very good for estimating state-of-charge and yet is actually an exact representation of state of charge of the battery cell. We run into some very serious problems if we try to use it as our only basis for estimating state-of-charge. Methods that do this are called coulomb counting because we're counting or measuring the number of coulombs that go into and out of a battery cell. There are several methods to estimate the SOC, in the next section we will be exploring the most common.

Battery Soc Methods

We can classify Battery Soc in five method branches: Conventional, Adaptive Filter Algorithm, Learning Algorithm, Non-Linear Observers and Others. The author is going to explain just the first two methods because the others are more complexed and sometimes less used.

Our application is to simulate cell dynamics in order to estimate SOC in a HEV battery pack. Several cell models have been proposed for SOC estimation. [10] presented many cell modelling methods in greater details for SOC estimation. The molecular level to design cell electrical dynamic model approach has been adopted in [11]. By using these models, accurate terminal voltage prediction achieved. However, measuring the many necessary physical parameters on a cell-by-cell basis in a high-volume consumer product couldn't considered. Other techniques such as cell modelling based on cell impedance over a wide range of ac frequencies at different states of charge have been involved in [12–16]. Least-squares fitted to measure impedance values yield model parameter values. SOC may be derived indirectly by calculating current cell impedance and comparing it to known impedance's at different SOC stages. No direct method was used for measuring impedance by injecting signals into cells.

Many papers represent equivalent circuit models for cells. To represent the open circuit voltage, [17–19] used voltage source or highly valued capacitor. The remaining circuit simulates the cell's intrinsic resistance as well as more dynamic effects such as terminal voltage relaxation. SOC can be calculated using a table lookup based on the OCV estimation. Here instead of SOC, OCV is fundamental state.
Coulomb counting is another method for SOC estimation. This is done by using open loop which is more sensitive to the measurement of current error. It is much accurate to the closed loop. [20] empirically designed feedback mechanism. Also, kalman filter technique can be used for feedback [3, 4].

Chapter 4

Methodology

4.1 Circuits Models

Open Circuit Voltage (OCV) is represented by a Controlled voltage source. The rest of the model include internal resistance of the cell and dynamic effects such as terminal voltage relaxation. The fundamental state used here is SOC instead of OCV and has similarities to circuit model.

For cell model, the only requirement is SOC to be constrain. SOC is denoted by "z_k" and is the member of the state vector x_k. To better understand of SOC, the following definitions are given as follows:

- When voltage v reaches v_h i.e $v = v_h$, cell is fully charged after being charged at infinitesimal current levels. The value of v_h at room temperature is 4.2 V.
- The cell is discharged, being drained at infinitesimal current levels. This occur at $v = v_1$ where v_1 = 3.2 V.
- A cell's capacity C is the highest amount of ampere-hours that can be taken from the cell until it is completely discharged at room temperature, beginning with the cell fully charged.
- At room temperature, number of ampere-hours that can be taken from the cell at the rate of C/30, beginning with fully cell charged is called Nominal capacitance C_n.
- Ratio of remaining capacity and nominal capacity is SOC of the cell. Remaining capacity is defined as: number of ampere-hours that can be taken from the cell before the cell fully charged at rate of C/30.

Based on the following definitions, SOC involving mathematical equations can be investigated.

$$z(t) = z(0) - \int_0^t \frac{\eta_i \, i \, \tau}{C_n} \tag{4.1}$$

where cell SOC is denoted by $z(t)$, instantaneous cell current is $i(t)$ and C_n is nominal cell capacity. η_i represents cell Coulombic efficiency. For charging it is equal is 1 and for discharging it is equal or less than 1. A discrete time approximate recurrence by using rectangular approximation for integration over time interval Δt ia written as:

$$z_{k+1} = z_k - \left(\frac{\eta_i \, \Delta t}{C_n}\right) i_k \tag{4.2}$$

Equation 4.2 is basic equation for including SOC. It is in the form of cell model state vector. i_k is the input here. Additional model and output state equation can be added in cell model as desired. Firstly an output equation is added from the literature [21] to check its validity and how enhancement can be made. Next, cell hysteresis and dynamics to model cell terminal voltage relaxation state is added. At the last, incorporating temperature dependence to the model.
We are taking models where SOC is taken as state. Here the state vector is $x_k = z_k$. SOC is only state in equation 4.3.

4.1.1 The combined Model

Terminal voltage can be predicted in different ways as SOC is now part of the model state. Other forms are adopted from [22] such as:
Shepherd model:

$$y_k = E_o - R\, i_k - \frac{K_i}{z_k}$$

Unnewehr universal model:

$$y_k = E_o - R\, i_k - K_i\, z_k$$

Nernst model:

$$y_k = E_o - R\, i_k - K_2\, ln(z_k) \; + K_3\, ln\,(1 - z_k)$$

where

- y_k = cell terminal voltage, R = internal resistance of cell. For different SOC levels, its different values can be used for charging and discharging.
- K_1, K_2, K_3 = constants for data fitting. K_i = polarization resistance.

All these terms collectively called ""the combined model". This combined model can perform better than the individual models. The combined model is presented as:

$$z_{(k+1)} = z_k - \left(\frac{\eta_i \, \Delta t}{C_n}\right) i_k \tag{4.3}$$

$$y_k = k_o - R\, i_k - \frac{K_1}{z_k} - K_2\, z_k + K_3\, ln(z_k) + K_4\, ln(1 - z_k) \tag{4.4}$$

By using system identification procedure, the combined model unknown parameters can be estimated. The advantage of this model is that its linearity in parameters and also that is, the unknowns occur linearly in the output equation.

$$Y = [y_1, y_2, ..., y_N]^T, \tag{4.5}$$

and the matrix

$$H = [h_1, h_2, ..., h_N]^T. \tag{4.6}$$

The rows of H are

$$h_j^T = [1, i_j^+, i_j^-, \frac{1}{z_j}, z_j, ln(z_j), ln(1-z_j)], \tag{4.7}$$

where i_j^+ is equal to i_j if $i_j > 0, i_j^-$ is equal to i_j if $i_j < 0$ else i_j^+ and i_j^- are zero. Then $Y = H\theta$, where $\theta^T = [K_0, R^+, R^-, K_1, K_2, K_3, K_4]$ is the vector of unknown parameters. Using a result from least-squares estimation theory, we solve for the parameters θ using the known matrices Y and H as $\theta = (H^T H)^{-1} H^T Y$ [23].

4.1.2 The Simple model

The components of the combined model can be further evaluated for more investigation. The output equation of the model is divided into two parts. One part based on SOC and other depend upon i_k:

$$y_k = fn(z_k) - fn(i_k) \tag{4.8}$$

where

$$fn(z_k) = k_o - R\,i_k - \frac{K_1}{z_k} - K_2\,z_k + K_3\,ln(z_k) + K_4\,ln(1-z_k)$$

and

$$fn(i_k) = R\,i_k$$

By Plotting the figure between $fn(z_k)$ and $fn(i_k)$ when the values are fit to parameters $K_o\ to\ K_4$ as shown in 4.1. The cell was completely charged first (constant current to 4.2 V). The cell was then discharged at a C/25 rate until it was fully discharged (3.0 V). After that, the cell was charged at a C/25 rate until the voltage reached 4.2 V. The low rates were used to keep the dynamics in the cells to a minimum. The OCV was calculated by averaging the cell voltage as a function of state of charge under discharge and under charge.

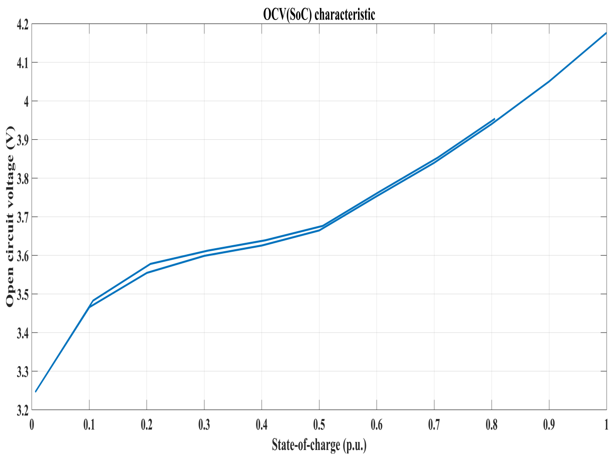

Figure 4.1: OCV (SOC)

The portion that is solely dependent on SOC deserves closer review. y_k, function of SOC, trying to attempting the OCV_{z_k} curve. More define form of the combined model can be implemented as:

$$z_{(k+1)} = z_k - \left(\frac{\eta_i\,\Delta t}{C_n}\right) i_k \tag{4.9}$$

$$y_k = OCV_{z_k} - R\,i_k \tag{4.10}$$

The output has been drawn from the equivalent model given by 4.2. Simple model composed of equa-

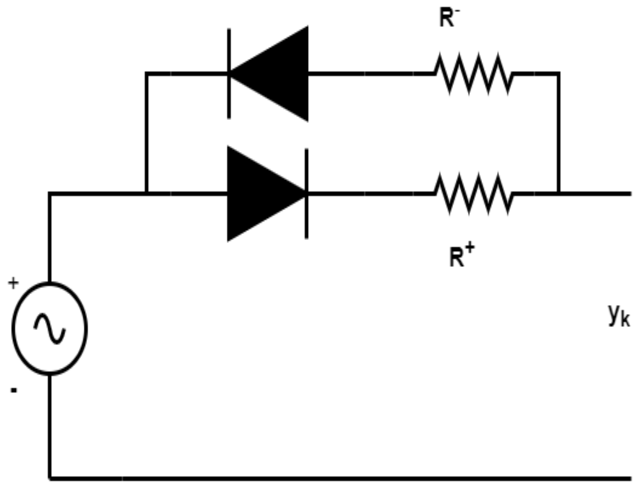

Figure 4.2: Equivalent circuit implemented by "simple" model, and approximated by "combined" model

tions 4.10, 4.14 and 4.3. Here the simple model is preferred because of it generalize form and less complex structure.This model type is also linear in the parameters. Off-line system identification is done as follows: We first form the vector

$$Y = [y_1 - OCV(z_1), y_2 - OCV(z_2, ..., y_n - OCV(z_N]^T, \tag{4.11}$$

and the matrix

$$H = [h_1, h_2, ..., h_N]^T. \tag{4.12}$$

The rows of H are

$$h_j^T = [i_j^+, i_j^-]. \tag{4.13}$$

Again, we see$Y = H\theta$, where $\theta^T = [R^+, R^-]$ is the vector of unknown parameters.We solve for the parameters θ using the known matrices Y and H as $\theta = (H^T H)^{-1} H^T Y$ [23].

4.1.3 The zero state hysteresis model

There are some flaws exposes in the combined and simple model such as subtle effect. In predicting SOC, it has serious consequences as shown in [21]. The cell voltage still relaxes to a value less than the true OCV for that SOC after a discharge. The cell voltage relaxes to a value greater than the true OCV for that SOC after a charge. This is not explained in previous models. Hysteresis model presented

this effect which occurs in cell.
In certain ways, the cell voltage lags behind the predicted voltage. It may also be described as a system property in which a change in the direction of the independent variable causes the dependent variable to fail to retrace the path it took in the forward direction. (For better understanding hysteresis phenomena, check [24]). The hysteresis model basic equations are:

$$z_{(k+1)} = z_k - \left(\frac{\eta_i \, \Delta t}{C_n}\right) i_k \tag{4.14}$$

$$y_k = OCV_{z_k} - s_k M(z_k) - R\, i_k \tag{4.15}$$

Sign of current is represented by s_k.

$$s_k = 1,\ for\ i_k > \epsilon,$$

$$s_k = -1,\ for\ i_k < -\epsilon$$

$$s_k = s_k - 1,\ for\ |i_k| \leq \epsilon$$

$M(z_k)$ is half the distance between the charge/discharge curve's two legs.This model type is also linear in the parameters. Off-line system identification is done as follows: We first form the vector

$$Y = [y_1 - OCV(z_1), y_2 - OCV(z_2, ..., y_n - OCV(z_N]^T, \tag{4.16}$$

and the matrix

$$H = [h_1, h_2, ..., h_N]^T. \tag{4.17}$$

The rows of H are

$$h_j^T = [i_j^+, i_j^-, s_j]. \tag{4.18}$$

Again, we see$Y = H\theta$, where $\theta^T = [R^+, R^-, M]$ is the vector of unknown parameters.We solve for the parameters θ using the known matrices Y and H as $\theta = (H^T H)^{-1} H^T Y$ [23].

4.1.4 The Thevenin Model

Fig. 4.3 shows the representation of the Thevenin model. It consists of certain electrical components such as R_o is internal resistance, R_p, C_p and V_p are the polarization resistance, capacitance and voltage respectively. y_k is the estimated terminal voltage of the battery. The mathematical representation of the thevenin model is given as:

$$y_k = OCV_{z_k} + V_p + IR_o \tag{4.19}$$

Where I is the current and its value is positive upon charging and negative when there is discharging mode. The equation for polarization voltage is determined by apply Kirchhoff's current at the node of parallel combination of polarization resistor and capacitor and is defined as:

$$\dot{V}_p = \frac{-V_p}{R_p C_p} + \frac{1}{C_p} I \tag{4.20}$$

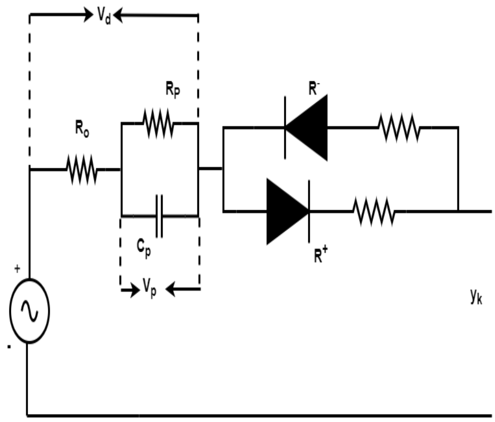

Figure 4.3: Equivalent circuit implemented by “Thevenin” model [25]

Applying transfer function to convert equation 4.20 into s-domain form:

$$y_k s = OCV(s) + \left(\frac{R_p}{R_p C_p s + 1} + R_o \right) I(s) \tag{4.21}$$

.One way to calculate the Thevenin parameters values is by using Recursive Least Square (RLS)[25]. In this project the author did not calculate them but took as references [2] .

4.1.5 The battery modeling challenges

As shown before, there are several ways to model the battery performances. The question to make ”is what are the biggest challenges in doing it”? Well, since we are modeling in an electrochemistry environment there are issues related to the chemistry of the material itself. We can identify three major challenges in modelling batteries.
Our model has to describes:

- SOC-dependent OCV;
- ohmic and diffusion voltages;
- hysteresis.

We are going now to address them one by one. We have seen as the battery can be described with electrical model with an OCV where simply Voltage at the terminal is equal to the OCV. Voltage is constant and is not function of current or past usage. At the same time, we notice how OCV changes according to change in SOC. For instance, when a cell is fully charged, its OCV is higher than when the cell is fully discharged. OCV depends on type of chemistry, temperature and indirectly also on SOC, Fig.4.4.

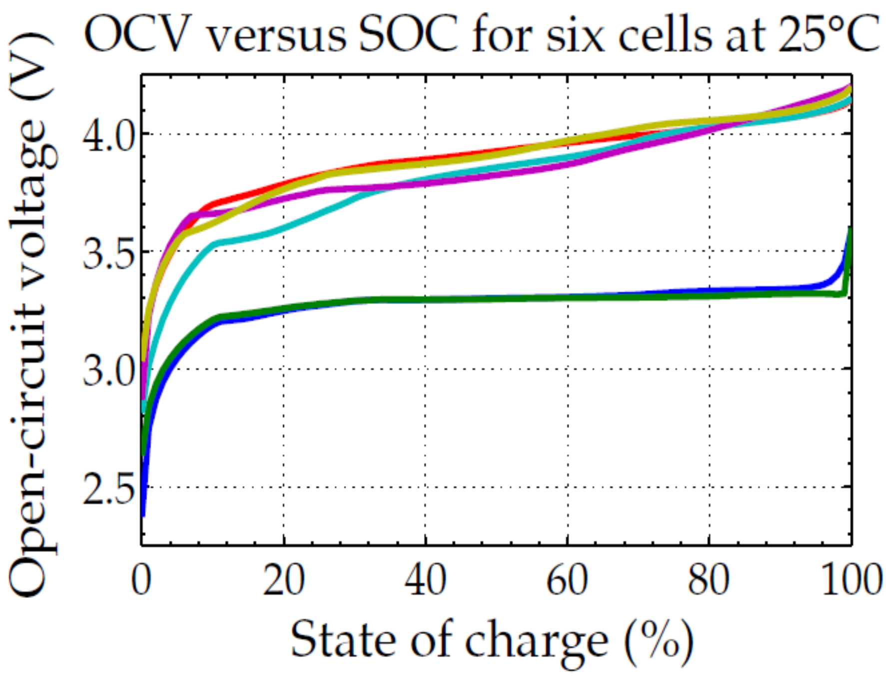

Figure 4.4: OCV-SOC different Lithium-ion battery chemistries[9]

When we instead take into consideration the variation of the voltage due to passage of current, we are talking about polarization effects. As we have seen with the simple model we can model the voltage's drop when the cell is under load, simply adding a resistance in series with the OCV like in fig.4.2 and described by the eq. 4.10 . Unfortunately, this models just the change of the instantaneous voltage. As we can see the in the fig.4.5 that shows the response in behaviour of the battery due to a discharge pulse followed by a battery rest .

In particular the voltage plotted in the fig.4.5 corresponds to the following scenario [9]:

1. the cell is at rest for the first 5min, and the voltage is constant;
2. the cell is then subjected to a discharge current pulse of constant magnitude fromt = 5min until t = 20min;
3. the load is removed, and the cell is allowed to rest for the remainder of the test.

The model explained so far explains the cell behaviour during the initial rest and the immediate voltage drop when current is applied and the immediate voltage recovery when the current is removed. $i(t)R_o$ in the eq. 4.10 predicts the instantaneous response to a current step. In the third period fig.4.5, when the cell rests we witness the dynamic response of the voltage . The voltage does not return to OCV but relax gradually. This phenomenon is seen as diffusion and can be modelled by adding a Rc branch in series that models the diffusion voltage as we have seen in Thevenin model. In the Randle circuit, Fig. 4.6 we can see the main variations in voltage to model.

This model is based on electrochemistry [9].

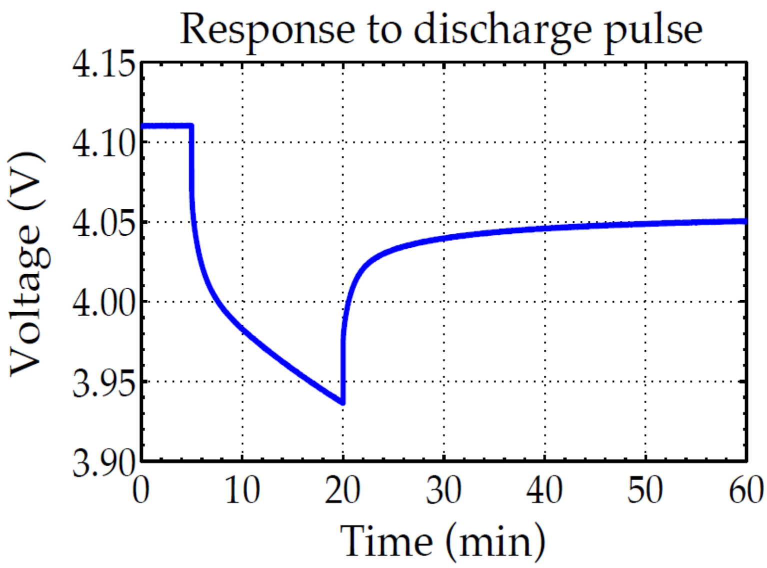

Figure 4.5: Response to discharge pulse[9]

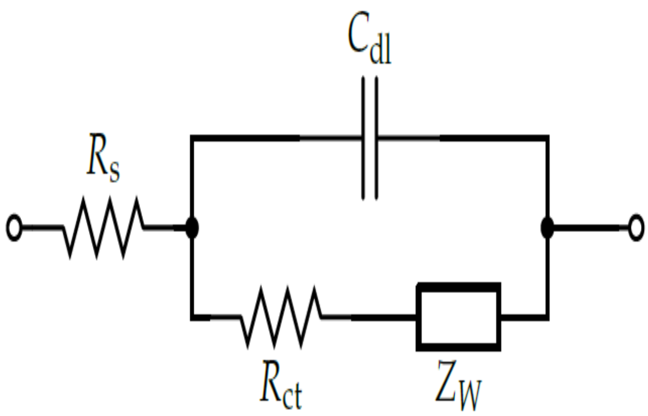

Figure 4.6: The Randle Circuit [9]

- R_s(Ro) models the electrolyte resistance;
- R_{ct} is charge-transfer resistance, models voltage drop over the electrode–electrolyte interface due to a load;
- C_{dl} is double-layer capacitance, models effect of charges building up in the electrolyte at electrode surface;
- Z_W is a Warburg impedance, models slow diffusion processes. $Z_W = A_W/\sqrt{j\omega}$

Warburg impedance is no easy to model with differential equation, instead it can be implemented using multiple resistor-capacitor networks in series. The double-layer capacitance is often omitted since has little impact on Randle circuit performances except at very high frequencies. So, everything can be reduced to Thevenin model Fig. 4.3.

However, there are not just these considerations to make when we models a Lithium-ion battery. For

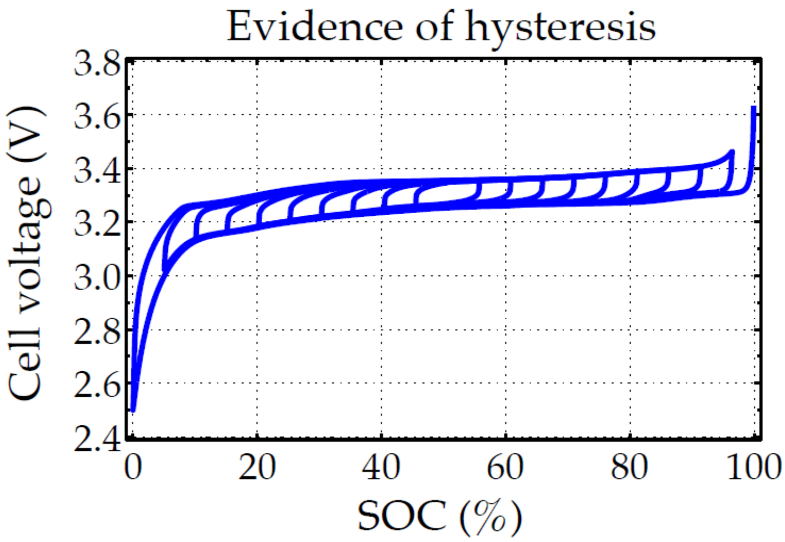

Figure 4.7: Hysteresis effect on a cell [9]

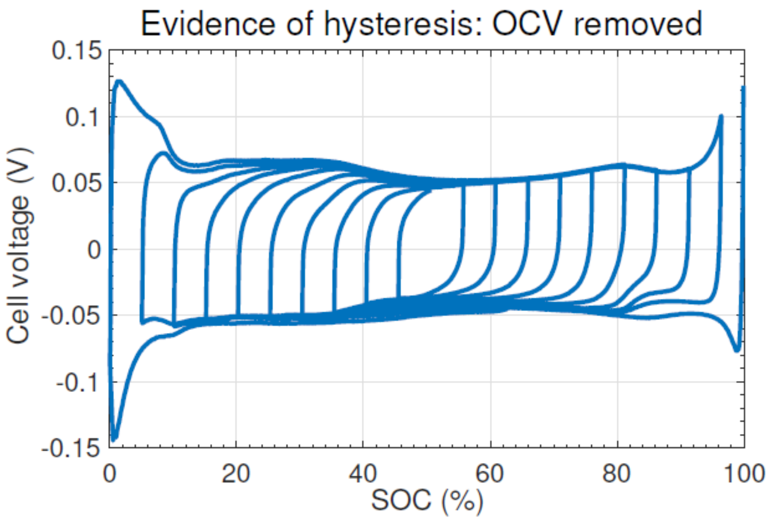

Figure 4.8: Hysteresis effect Ocv removed [26]

example, when we leave the cell to rest long enough, diffusion should decay to zero and the model voltage to OCV. This is not the case. Indeed, for every SOC, there is a range of possible stable "OCV" values. In the Fig. 4.7 it can be seen the presence of hysteresis for C/30 (approximate equilibrium) test. We must consider it because otherwise can causes large prediction errors. To be noticed is that the diffusion voltages change directly with time but hysteresis change when SOC changes. To get a better idea of what hysteresis is, we subtract OCV from the prior results. So, in Fig. 4.8 we can see there is a maximum plus/minus hysteresis, may be SOC dependent: $M(z, \dot{z})$. The eq .4.15 shows together with the Fig. 4.8 that Hysteresis, plotted versus SOC, "decays" towards $M(z, \dot{z})$ at a rate that depends on how close it presently is to that amount. Finally, we observed that Hysteresis is a path-dependent voltage that does not decay to zero when the cell rests, unlike diffusion voltages.

Chapter 5

Study case

5.1 Battery specifics

The battery data used in this project belong to an open source Center for Advanced Life Cycle Engineering (CALCE), University of Maryland [2] .

The tested battery is the INR 18650-20R a $LiNiMnCoO_2/Graphite$ lithium-ion cells. In the Tab. 5.1 the parameters of the battery are shown. In order to test the battery the following facilities were needed, Fig. 5.1 : the test sample collocated inside a Temperature Chamber that kept the Temperature constant to perform three different tests at three different temperature on the battery test bench at 0 °C, 25*C and 45*C; an Arbin BT2000 battery test system; a PC with Arbin software to monitor data information and to set up orders such as charging and discharging. The time interval at which all the data were measured and saved is 1s.

Battery (Parameters)	Specifications (Value)
Capacity Rating	$2000mAh$
Cell Chemistry	LNMC/Graphite
Weight (with safety circuit removed)	$45.0g$
Dimensions (mm)	$18.33 \pm 0.07mm$
Nominal voltage	$3.6V$
Maximum current	$22A(at25^oC)$
Usage temperature	$0 - 50^oC$

Table 5.1: INR 18650-20R parameters [2]

Incremental OCV test

To perform the Incremental OCV test many SOC Intervals and rest periods were taken after those the OCV with the related SOC were compared. The missing data points were obtained through interpolation. According to [2] the battery cell underwent through the following Incremental OCV Test

- 1 Charge battery to cut-off voltage of 4.2V at constant current of 1C-rate
- 2 Charge at constant voltage until its current is reduced to 0.01C
- 3 Now Discharge at constant rate of C/20 until the voltage drops to 2.5V
- 4 Fully Charge at constant rate of C/20 to 4.2V
- 5 Average voltage of charging and discharging process recorded as OCV at 0℃, 25℃ and 45℃

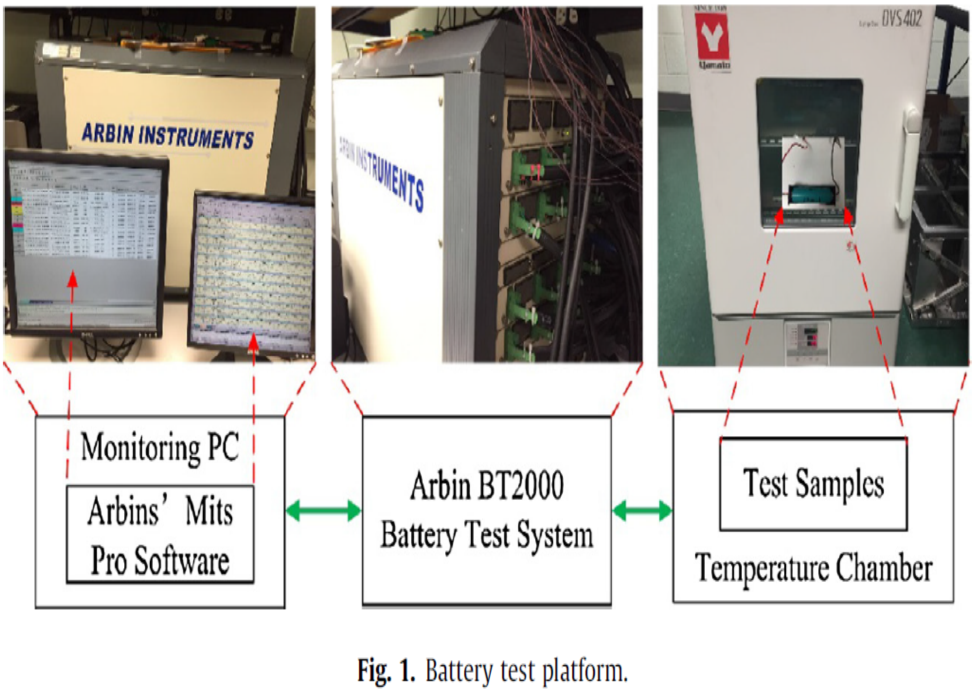

Figure 5.1: Simulink block for BMS [2]

In the Fig. 5.2 is shown the test Profile of the incremental OCV test performed by [2]. Ten charging pulses at every 10% SOC followed by other ten discharging pulses. The rest time set was two hours were the battery cell was allowed to rest.

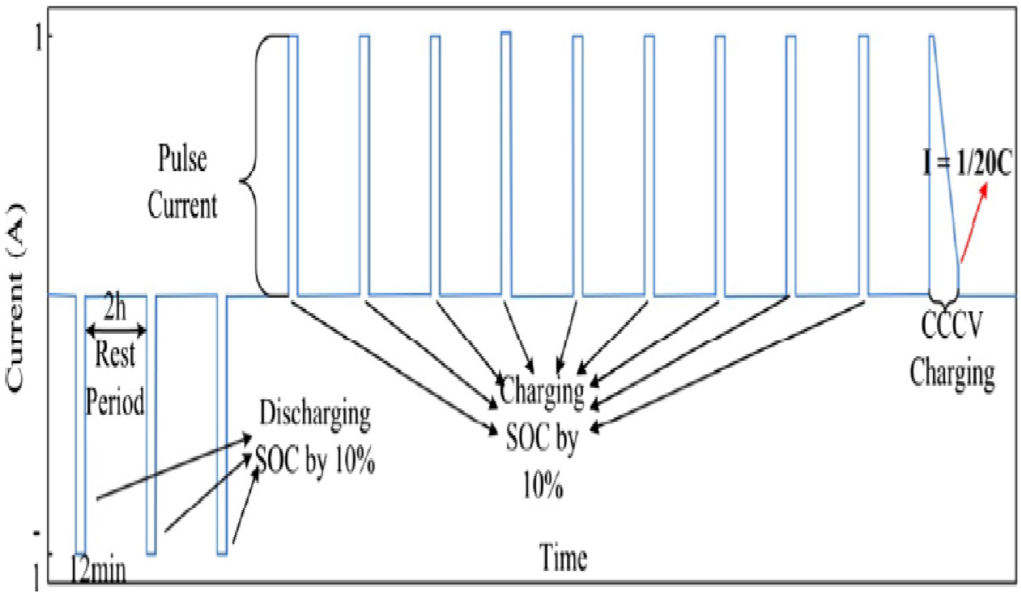

Fig. 3. Test profile of the incremental OCV test.

Figure 5.2: Test profile of the incremental OCV test [2]

5.2 Input data, tools adopted and results

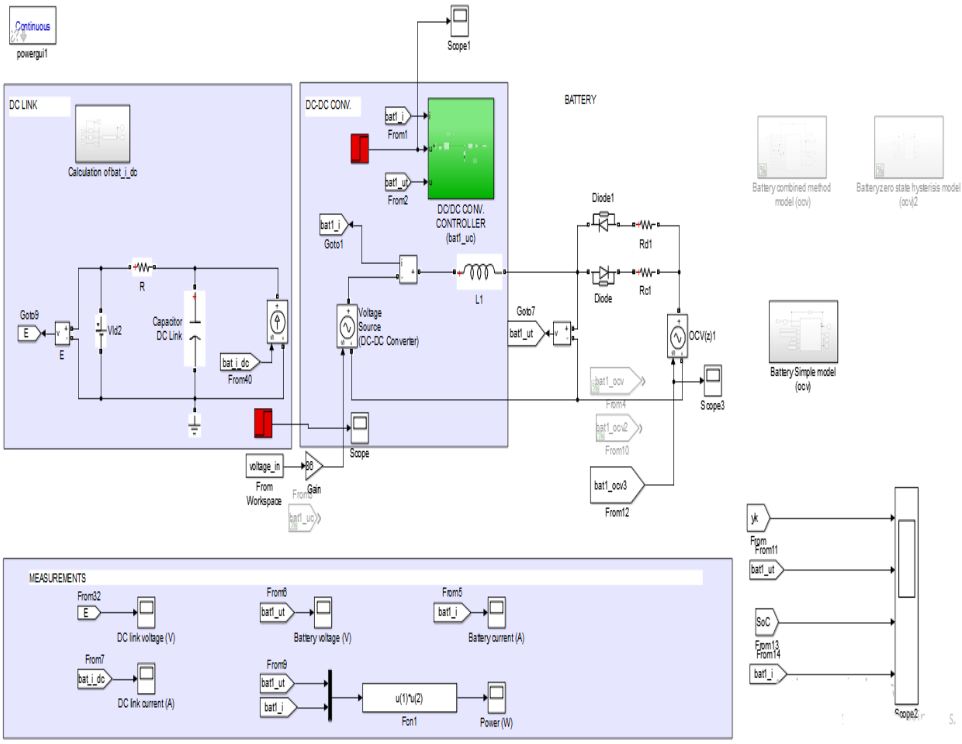

Figure 5.3: Simulink block for BMS

The MATLAB/Simulink-based environment has been used for showing performance of the circuit models: The simple model, The combined model and The zero-state hysteresis model given by equations 4.3, 4.10 and 4.14 for the simple model, equations 4.3 and 4.4 for the combined model and equations4.14 and 4.15 for the zero state hysteresis model and equation 4.21 for thevenin model. The goal is to have the cell model output resemble the cell terminal voltage under load as closely as possible, at all times, when the cell model input is equal to the cell current. The simulink block for BMS along with circuit models has been presented in 5.3. R_{d1} and R_{c1} are the discharging and charging resistance of the battery. Battery model used here is Lithium-ion and its single cell parameters are given in table 5.2. For every SOC lookup vaues, values of OCV will be calculated in table 5.3. The Cell Thevenin Resistance and Capacitance were extrapolated from the previous tests and model at [2].

The pack parameters for lithium-ion battery are given in table 5.8 The discharging resistance of the pack battery is the combination of single cell resistance and ratio of series and parallel cells of the battery. The number of series and parallel combination of cells are 86 and 44 respectively. Similarly other parameters details such as pack charging resistance ($R_{c_{pack}}$), cell capacity pack ($Bat1\ C_{n_{pack}}$), SOC lookup table in case of pack ($bat1\ OCV\ lookup - table_{pack}$), ($bat1\ Unom_{pack}$), ($bat1\ Uexp_{pack}$), ($bat1\ Umin_{pack}$) are given below:

$$R_{d_{pack}} = R_{d1} * \frac{Bat1.Nseries}{Bat1.Nparallel}$$

Parameter	Symbol	Value
R_{d1}	Discharging resistance	0.125
R_{c1}	charging resistance	0.115
Coulomb efficiency	Bat1.eta	1
Time step	$Bat1.Delta_t$ (s)	0.01
Cell capacity	$bat1.C_{n_{cell}}$ (As)	7200
Cell Thevenin capacitance	$cap.thevenin$ (F)	1127.6
Cell Thevenin resistance	$res.thevenin$ (Ohm)	0.00345

Table 5.2: Lithium ion single cell parameters

SOC	OCV
0.0066	3.2472
0.1004	3.4658
0.2004	3.5546
0.3003	3.5987
0.4002	3.6254
0.5002	3.6645
0.6001	3.7531
0.7000	3.8397
0.8000	3.9400
0.8999	4.0502
0.9998	4.1763

Table 5.3: SOC and OCV lookup table

$$R_{c_{pack}} = R_{c1} * \frac{Bat1.Nseries}{Bat1.Nparallel}$$

$$Bat1\ C_{n_{pack}} = \ bat1.C_{n_{cell}} * Bat1.Nparallel$$

$$Bat1\ OCV\ lookup - table_{pack} = \ Bat1.Nseries* \\ [OCV\ values\ from\ table.2]$$

$$Bat1\,Unom_{pack} \ = \ mean * (Bat1\ OCV\ lookup - table_{pack})$$

$$Bat1\,Uexp_{pack} \ = \ max * (Bat1\ OCV\ lookup - table_{pack})$$

$$Bat1\,Umin_{pack} \ = \ min * (Bat1\ OCV\ lookup - table_{pack})$$

The set points and initial conditions for running simulation to estimate the terminal voltage (y_k) are given as:

$$Bat1.initial_z \;=\; 0.7$$

$$Bat1.initial_{OCV} \;=\; interpl(bat1\ OCV\ lookup - table_{pack},$$
$$bat1\ OCV\ lookup - table, Bat1.initial_z)$$

This section consists of four further subsections. Subsection 5.2.1 explains how the Dc- Link and Dc-Dc Converter are modelled. Subsection 5.2.2 shows the simulation performance of the simple model in term of estimated terminal voltage, actual voltage, charging/discharging current and SOC. Similarly subsection 5.2.3 shows behavior of the combined cell for said properties discussed earlier. Simulation discussion for the zero state hysteresis model and Thevenin model is done in subsection 5.2.4 and 5.2.5 respectively.

5.2.1 Dc-Link DC-DC Converter

In this section the charger associated to model battery pack is shown. In particular, the author used as reference [27, p. 316] to model the dc-dc converter as a controllable voltage source . This model also presents a controller which determines the voltage magnitude at terminal of this voltage source. In the Fig. 5.4is shown the DC link block and in Tab. 5.4 the parameters used. The Dc voltage source is initialized at dc.E, R = 1e-5 Ohm, with capacitance dc.C and initial voltage dc.E. The initial amplitude for the current source, 0A [27, p. 316].

In Fig. 5.5 is shown the inside calculation of $bat_{i_{dc}}$. The initial condition for the memory block is dc.E.

Parameter	Symbol	Value
Rated dc-link voltage	dc.E	800 (V)
DC-link Capacitance	dc.C	0.01 (F)
Resistance dc-link	R	1e-5 (Ohm)

Table 5.4: Dc link parameters

Parameter	Symbol	Value
Inductance between converter and battery	bat1.L	0.005 (H)
Rated Power	bat1.P	20e3 (W)
Maximum admissible current (battery side)	$bat1.Irated$ = $bat1.P$ / $bat1.Uexp\_pack$	(A)

Table 5.5: Dc-Dc converter parameters

In Fig. 5.6 is shown the DC-DC converter Block and in Tab. 5.5, its parameters. The voultage source should be initialized at $bat1.initial\_ocv$; the inductance is bat1.L, with 0 A as the initial current;

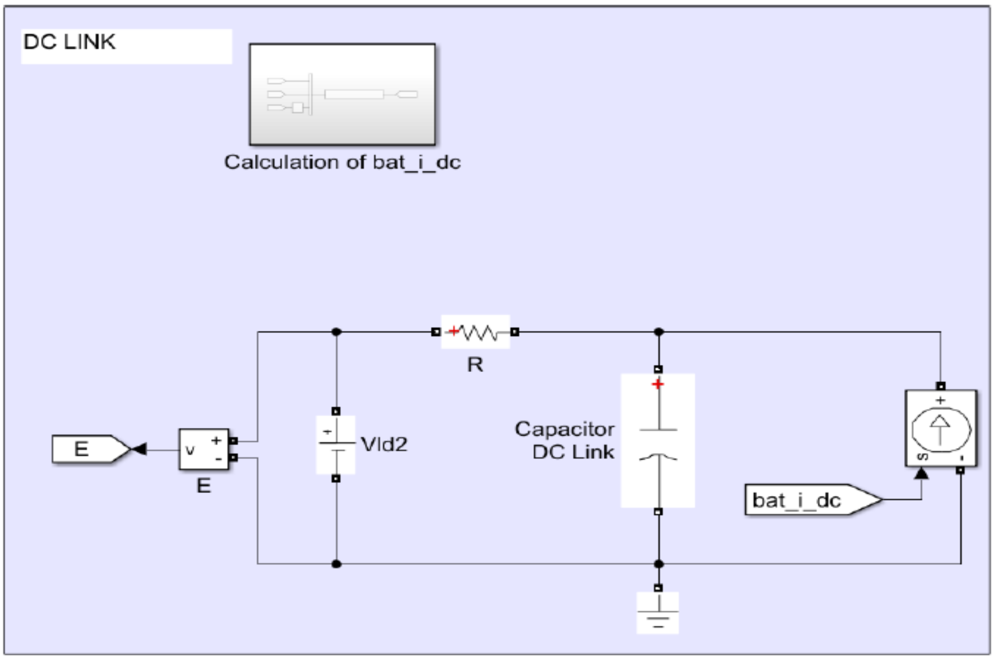

Figure 5.4: DC link block

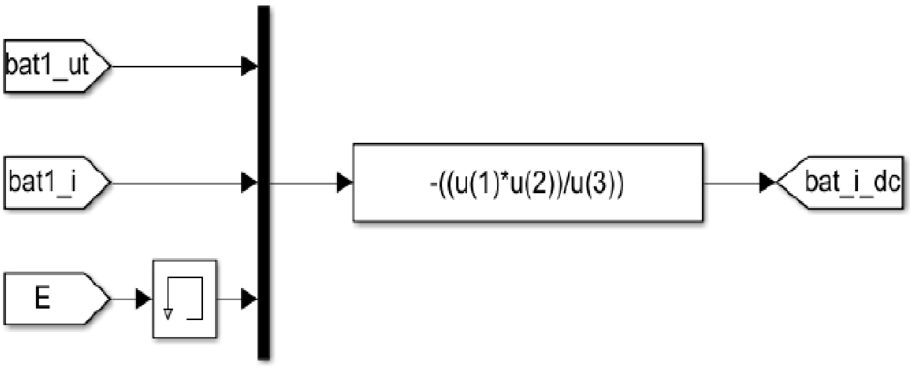

Figure 5.5: Inside calculation of $bat_{i_{dc}}$ block.

the step profiled setpoint should consider (step time : bat1.voltage_setpoint_step_time; initial value: bat1.voltage_setpoint_step0; final value : bat1.voltage_setpoint_step1; sample time 0) [27, p. 316]. In Fig. 5.7, 5.8, 5.9 and 5.10 are shown the DC/DC converter controller. In Fig 5.9 the initial value for the integrator is 0. The upper limit for the saturation block is bat1.Irated and the lower, bat1.Irated [27, p. 316]. In Fig.5.10 the initial value for the integrator is $bat1.initial_{ocv}/dc.E * 0.99$ [27, p. 316].

Parameter	Symbol	Value
Natural frequency	bat1.wu	1 (rad/s)
Damping coefficient	bat1.xiu	0.7

Table 5.6: Voltage controller parameters to be selected by the designer

Calculation for Voltage Controller

$bat1.Kpu = 2 * bat1.xiu * bat1.wu * bat1.C$; % (-) - Proportional control gain

$bat1.Kiu = bat1.wu^2 * bat1.C$; % (-) - Integral control gain

Parameter	Symbol	Value
Natural frequency	bat1.wi	20 (rad/s)
Damping coefficient	bat1.xii	0.7

Table 5.7: Current controller parameters to be selected by the designer

Calculation for Current Controller

$bat1.Kpi = 2 * bat1.xii * bat1.wi * bat1.L/dc.E$; % (-) - Proportional control gain

$bat1.Kii = bat1.wi^2 * bat1.L/dc.E$; % (-) - Integral control gain

Battery voltage set points

$bat1.voltage\_setpoint\_step\_time = 600$;

$bat1.voltage\_setpoint\_step0 = bat1.initial\_ocv$;

$bat1.voltage\_setpoint\_step1 = bat1.Uexp\_pack$; In Tab. 5.6 and 5.7 are shown the parameters for the voltage and current controllers respectively.

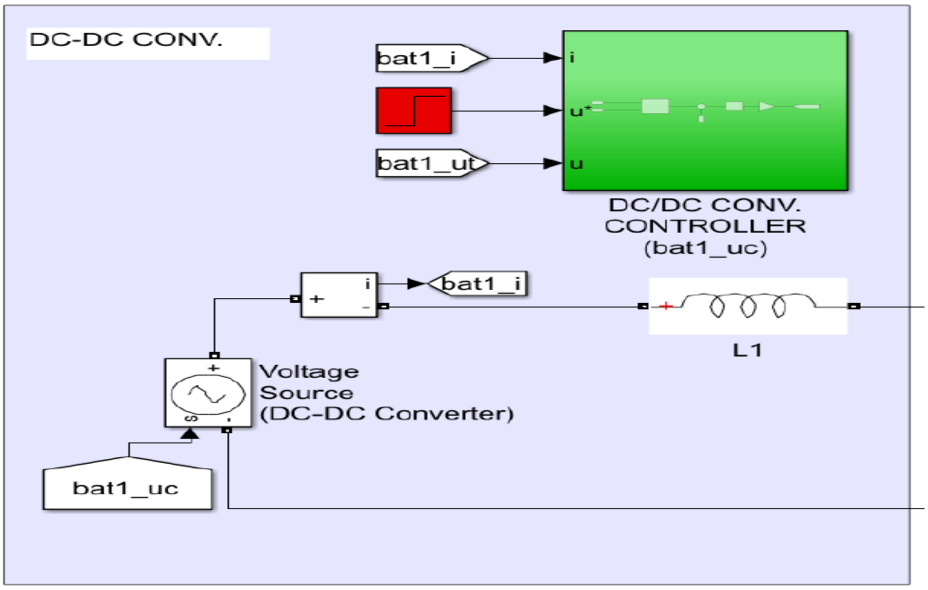

Figure 5.6: DC-DC converter Block

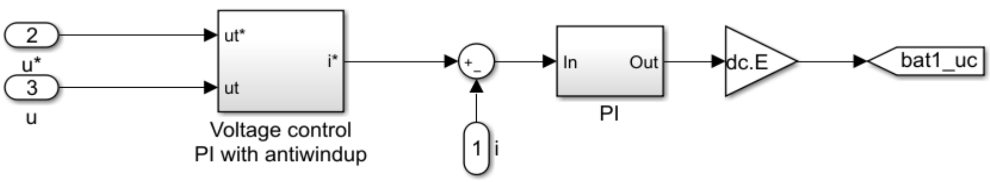

Figure 5.7: Inside the block Dc-Dc Coverter block $(bat1_uc)$

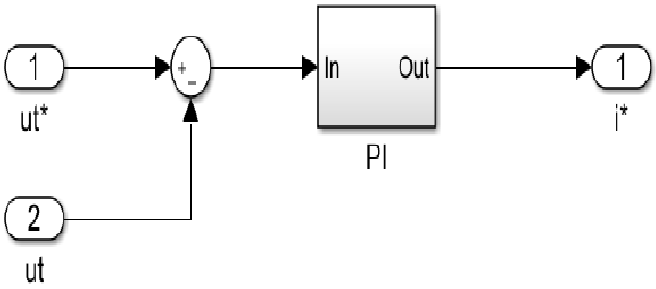

Figure 5.8: Inside the block Dc-Dc Coverter block $(bat1_uc)$ Voltage control PI with antiwindup

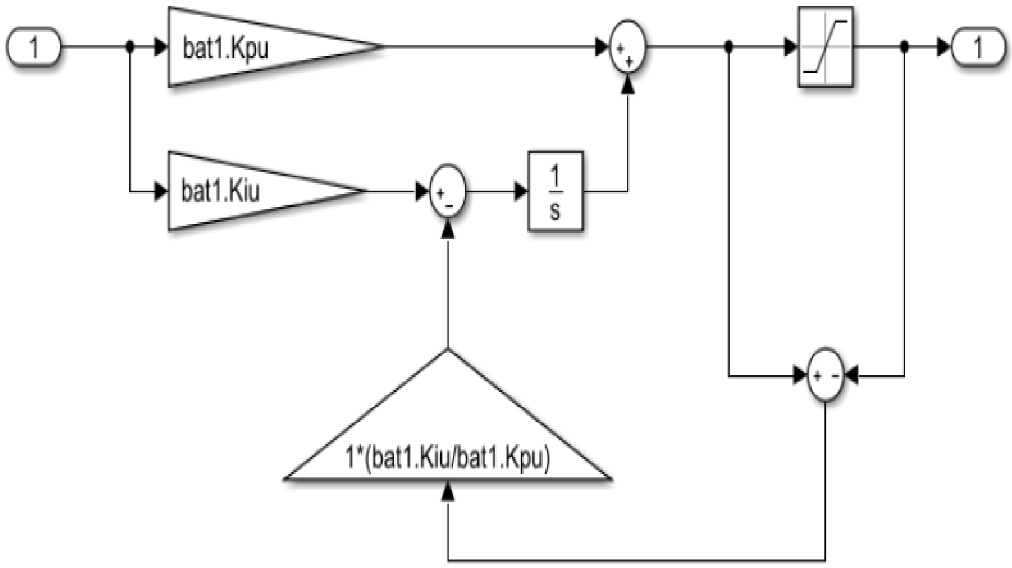

Figure 5.9: Inside the block Dc-Dc Coverter block $(bat1_uc)$ Voltage control PI with antiwindup PI

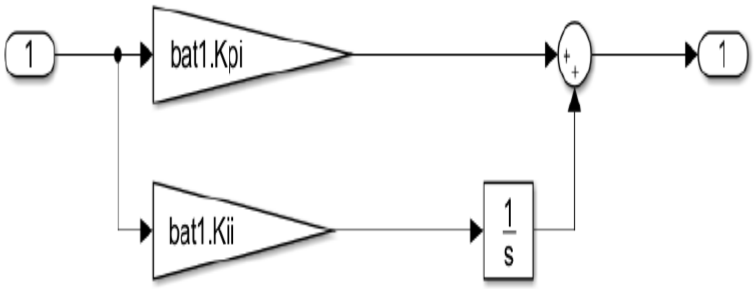

Figure 5.10: Inside the block Dc-Dc Coverter block $(bat1_uc)$ PI

5.2.2 The simple model

Here, the performance of the the simple model has been done. The simulink model for equations 4.9 and 5.11 are shown in fig. 5.12 The model parameters used for the implementation of the Simple model is given in Tab.5.8.The parameter has been calculated by using off-line system identification with eq. 4.11, 4.12 and 4.13.

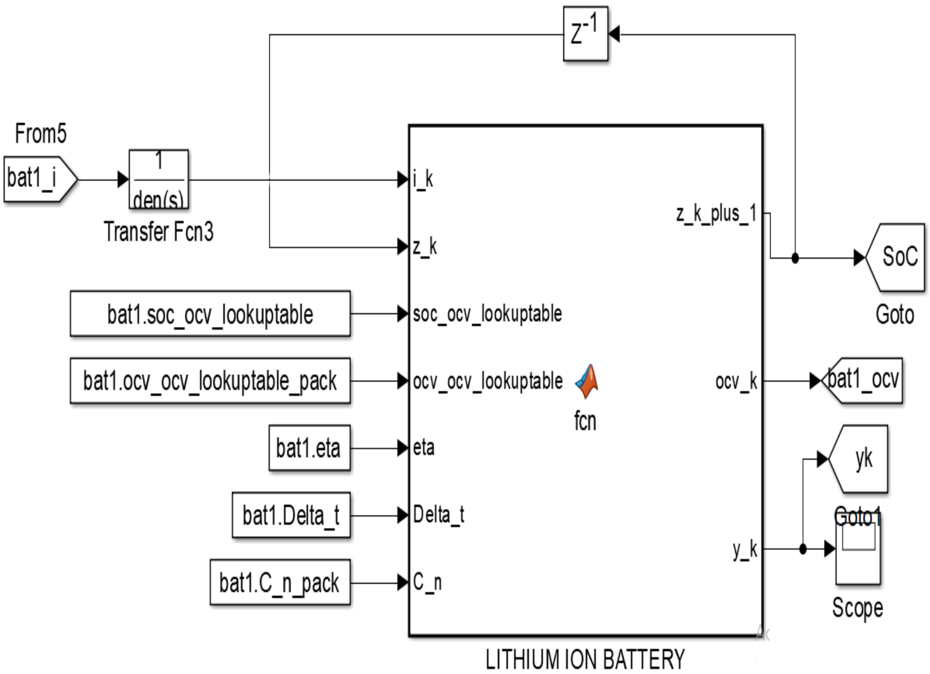

Figure 5.11: The simple model simulink block

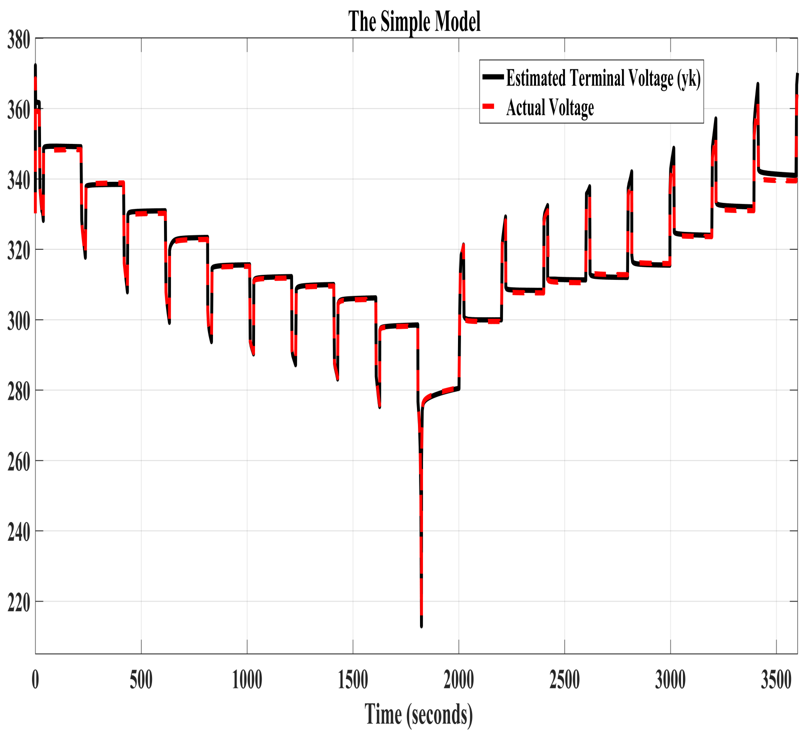

Figure 5.12: Terminal estimated Vs actual voltage

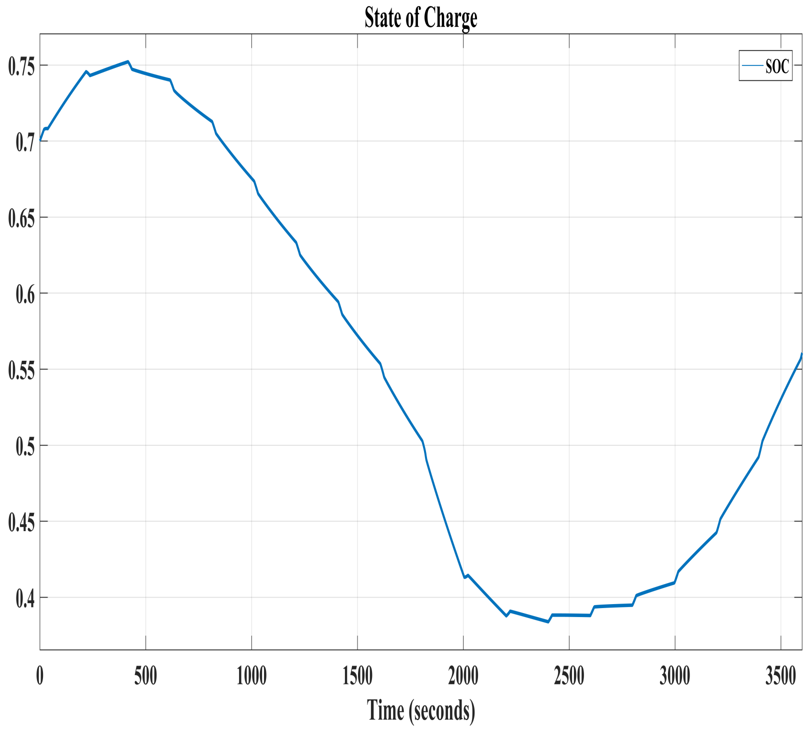

Figure 5.13: SOC of the Simple model

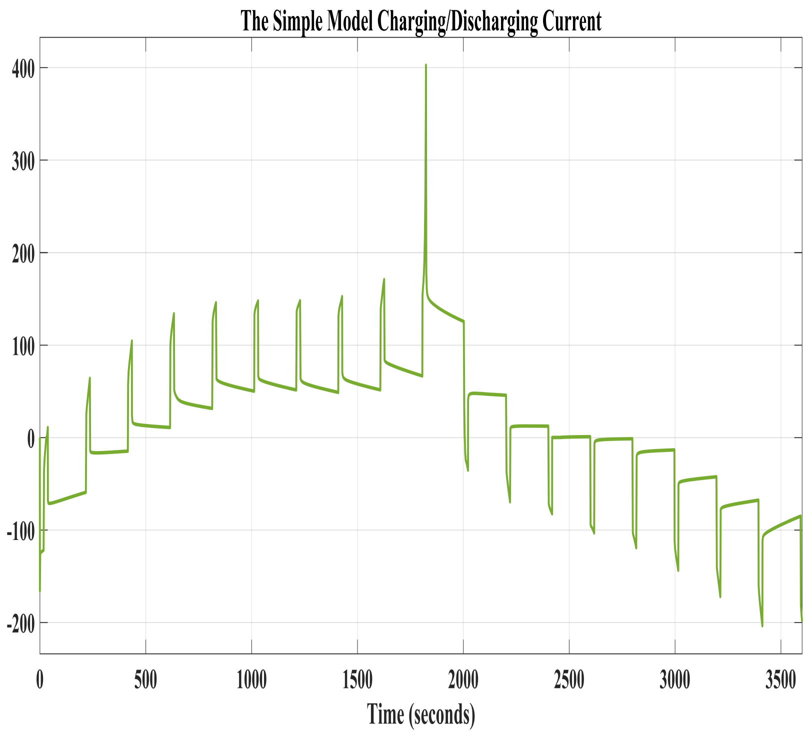

Figure 5.14: Charging/Discharging Current of the Simple Model

Parameter	Value
R	0.253091021257146

Table 5.8: Circuit Model parameters

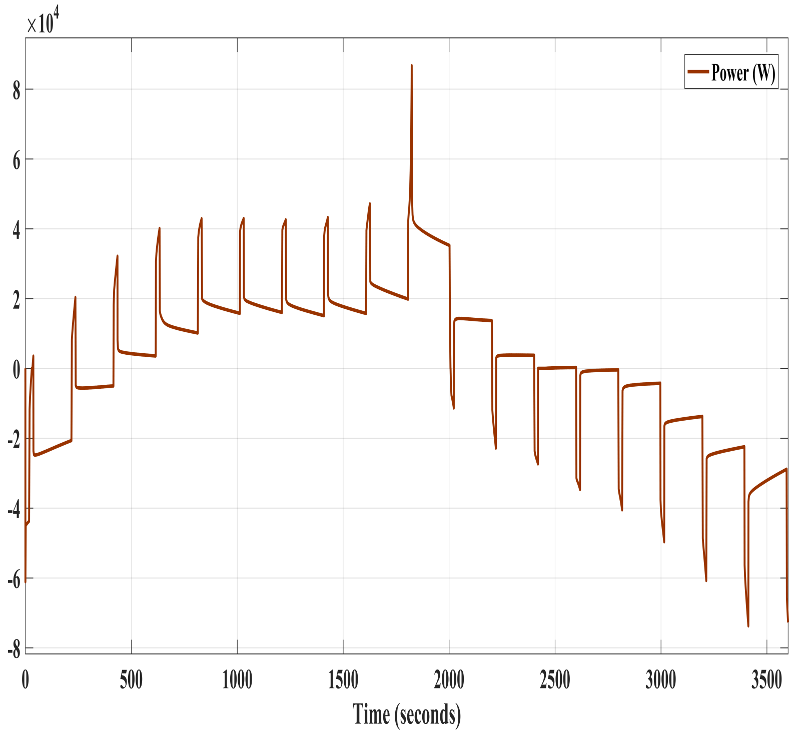

Figure 5.15: Power of the Simple Model

5.2.3 The Combined Model

Here, the performance of the Combined model has been done. The simulink model for equations.4.3 and 4.4 are shown in fig. 5.16.The model parameters used for the implementation of the Combined model is given in Tab.5.9.The parameters has been calculated by using off-line system identification with eq. 4.5, 4.6 and 4.7.

Parameter	Value
k0	3.22901051353494
R	0.253091021257146
k1	0.00301866406686573
k2	-0.803016645948219
k3	-0.0907895654362170
k4	-0.0248733178576978

Table 5.9: Circuit Model parameters for The Combined Model

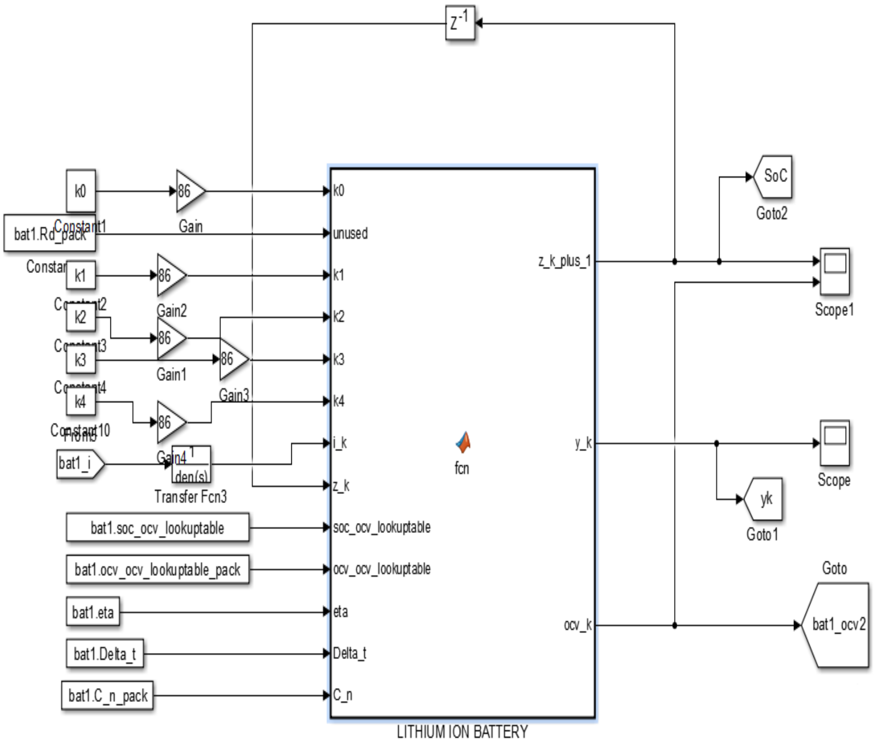

Figure 5.16: The combined model simulink block

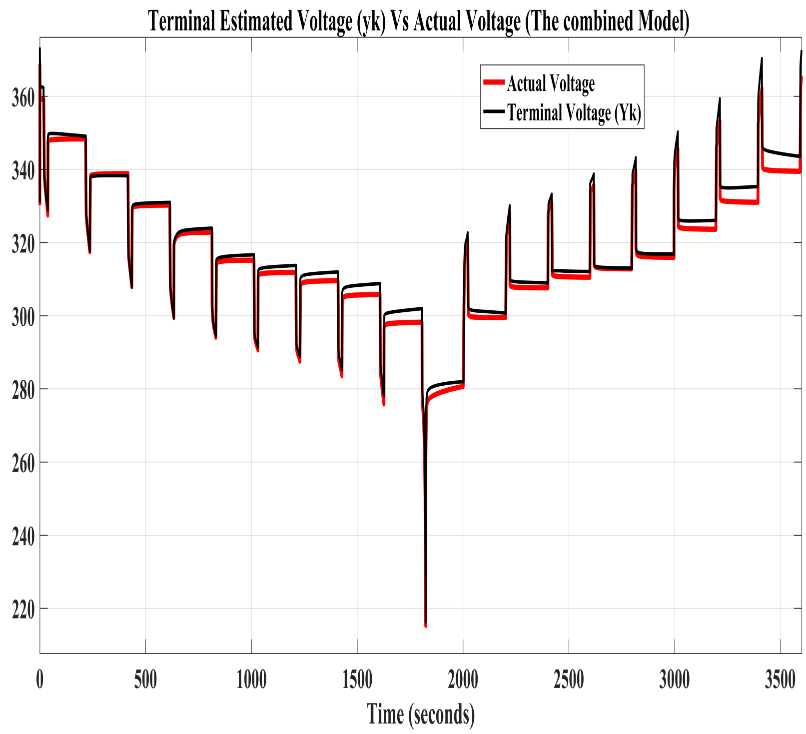

Figure 5.17: Terminal Voltage (yk) vs actual voltage of the Combined Model

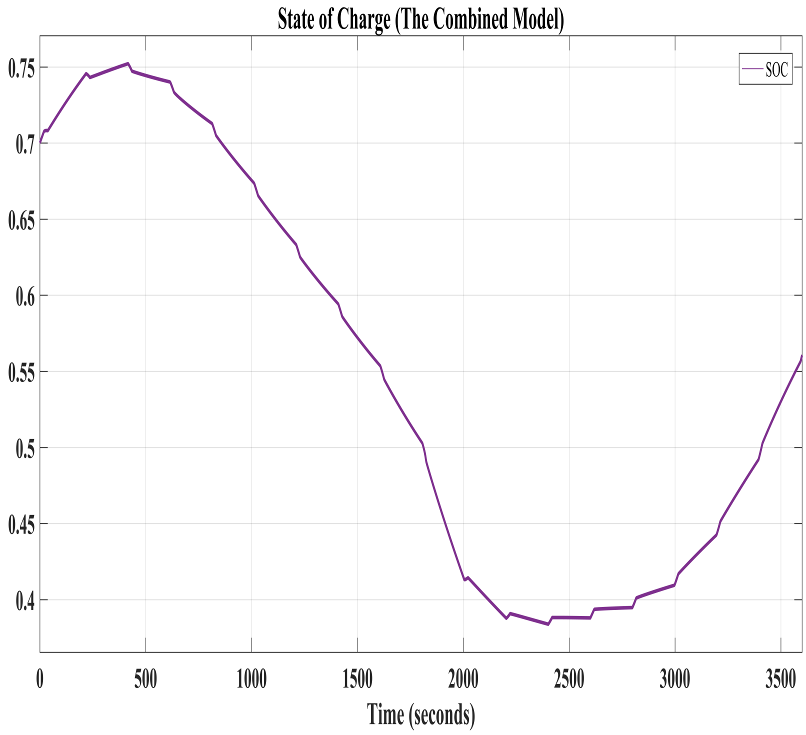

Figure 5.18: SOC of the Combined Model

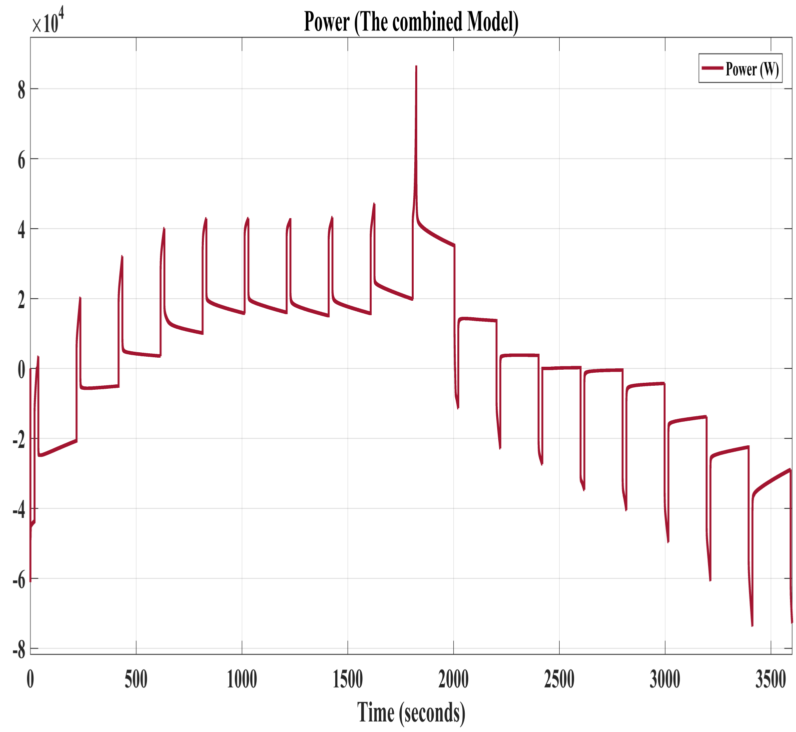

Figure 5.19: Power of the Combined Model

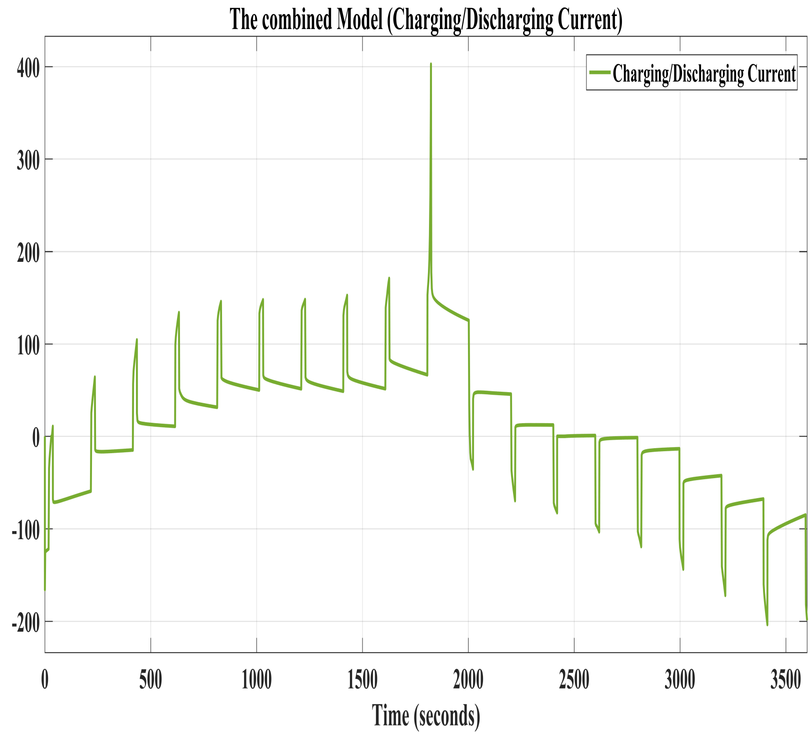

Figure 5.20: Charging/Discharging Current of the Combined Model

5.2.4 The zero state Hysteresis Model

The implementation of the zero state hysteresis model has been done in this section. The simulink model for equations. 4.14 and 4.15 are shown in fig. 5.21. The model parameters used for the implementation of the zero state Hysteresis model is given in Tab.5.10.The parameters has been calculated by using off-line system identification with eq. 4.16, 4.17 and 4.18.

Parameter	Value
R	0.253091021257146
M	-0.00188930759029581

Table 5.10: Circuit Model parameters for The zero-state Hysteresis Model

5.2.5 The Thevenin model

Here introducing thevenin model consisting of thevenin resistance and capacitance in battery which are not been calculated from the author. The model parameters have been extracted by the following paper which worked on the same battery pack [2]. In this section the author used the thevenin circuit model, which is made by adding a RC block to the equivalent model, implementing it for each model previous tested. In fig. 5.27 the voltage estimations of each model has been shown and compared to the actual voltage.

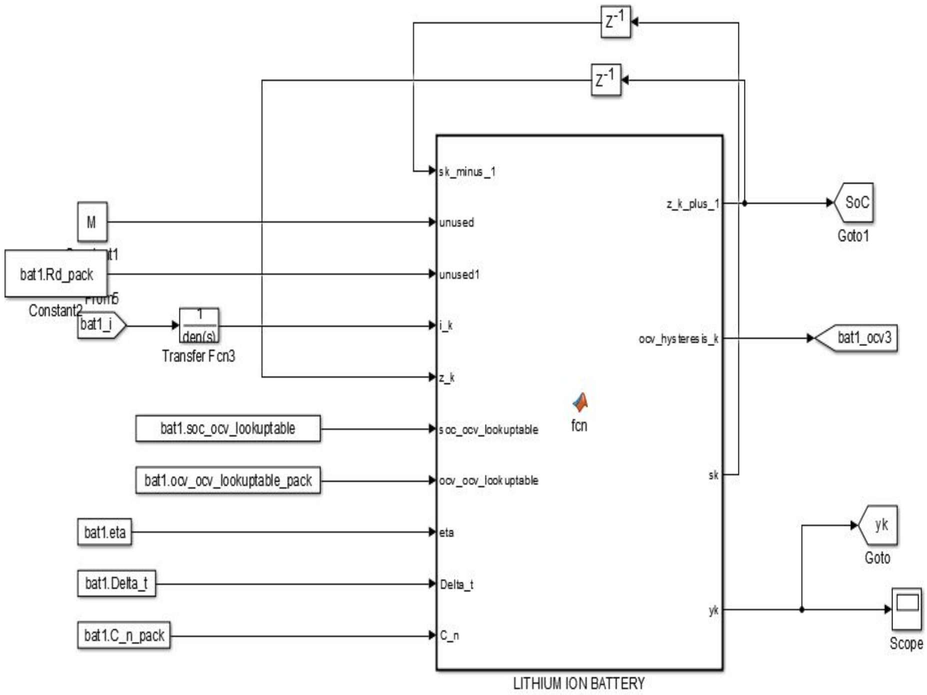

Figure 5.21: Simulink model zero hysteresis model

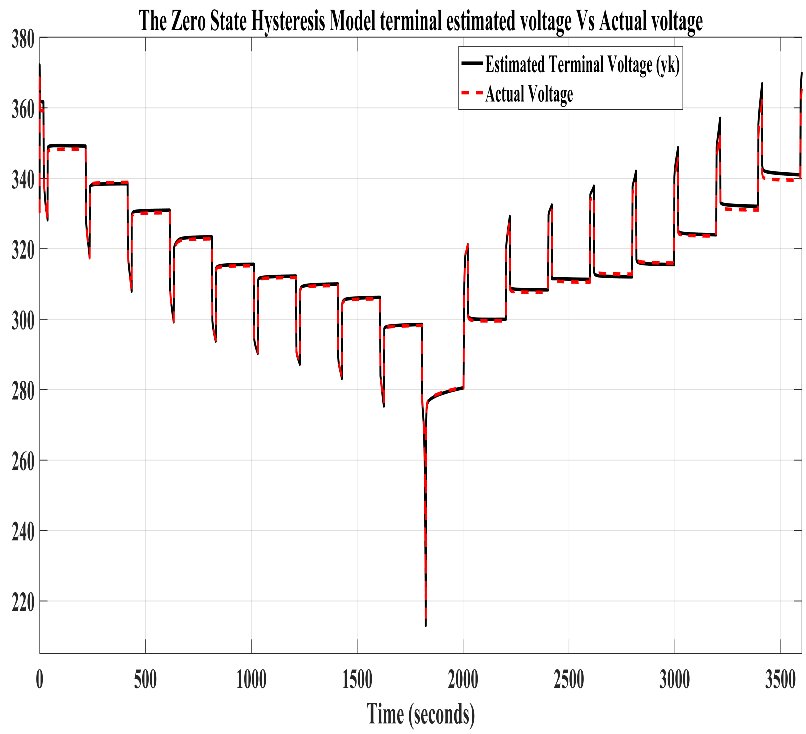

Figure 5.22: Terminal voltage Vs Actual Voltage of the zero state Hysteresis Model

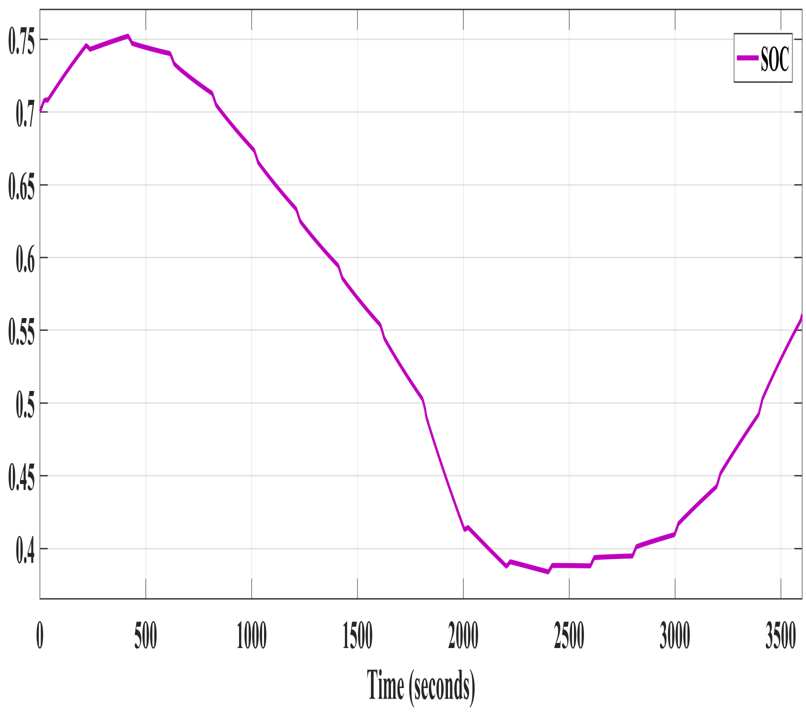

Figure 5.23: SOC of the zero state Hysteresis Model

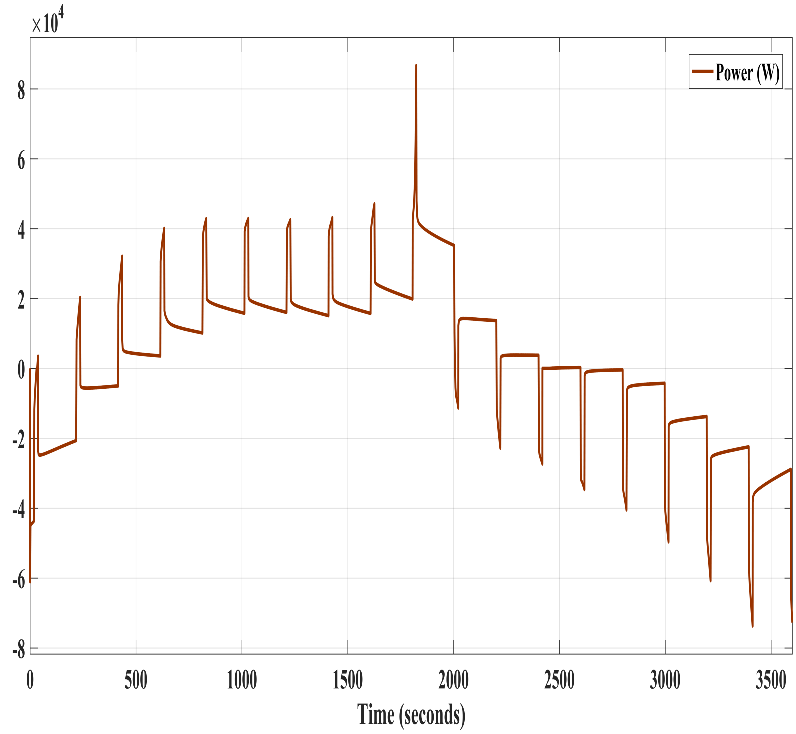

Figure 5.24: Power of the zero state Hysteresis Model

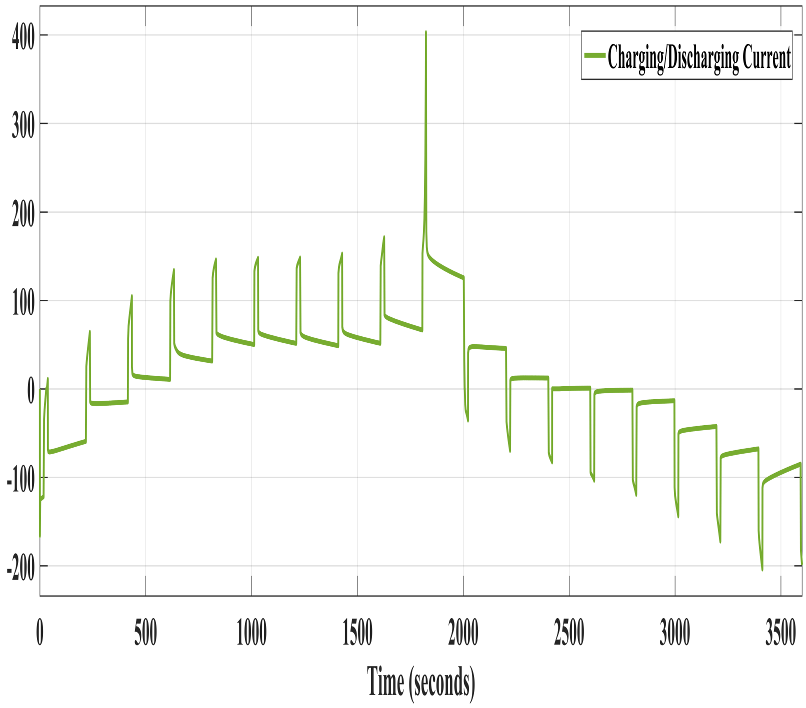

Figure 5.25: Charging and Discharging Current of the zero state Hysteresis Model

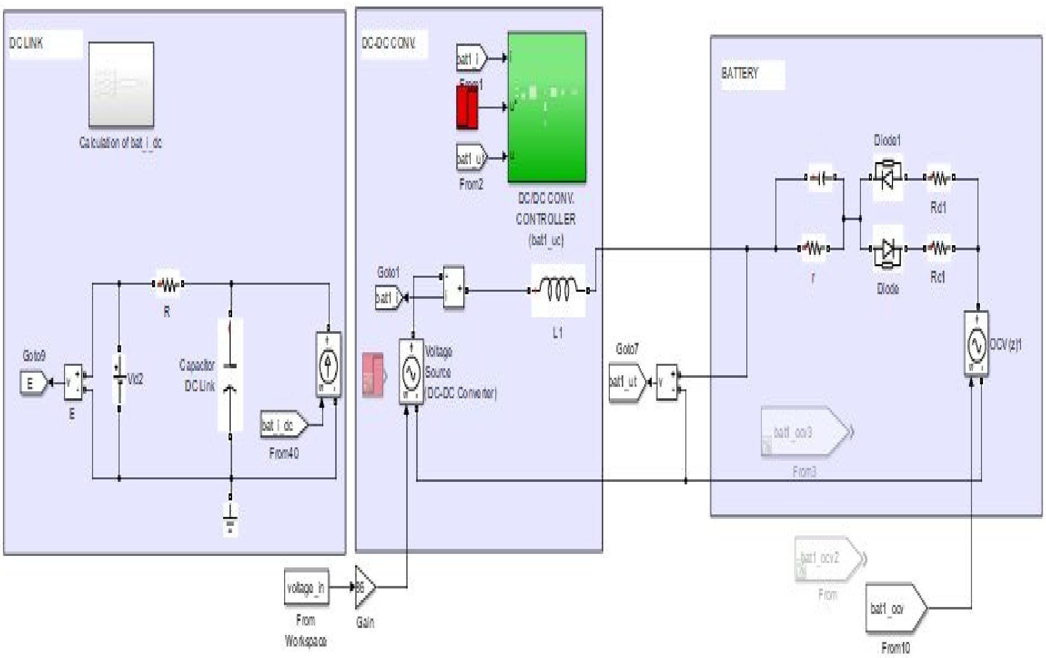

Figure 5.26: BMS Simulink block with thevenin circuit

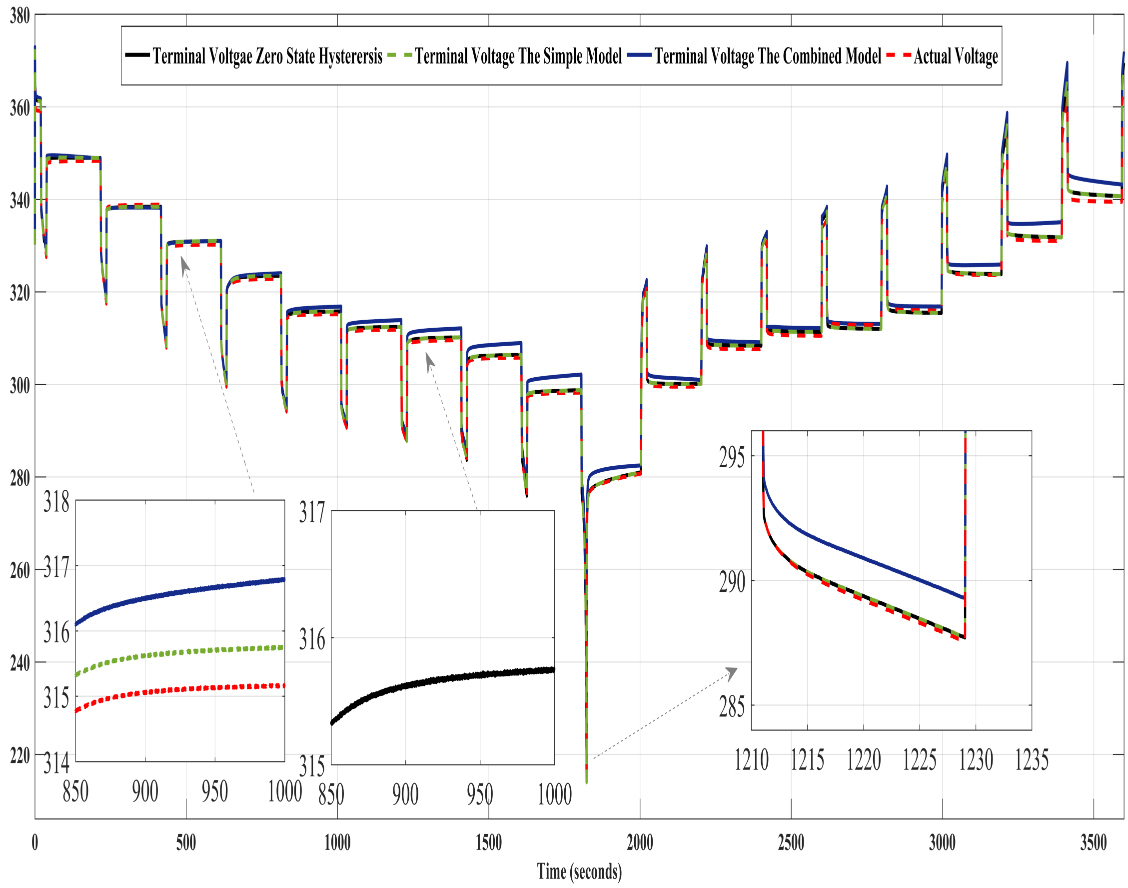

Figure 5.27: Terminal estimated Voltage Vs Actual Voltage: Thevenin Model implenting and comparing all the other three models

Chapter 6

Discussion of results

In this chapter the author discussed the Results in the prior chapter, analyzing the several data and graphs generated by the project.

6.1 The Simple model

In fig. 4.2, y_k is the terminal estimation voltage which is the required goal of the model to achieve it as same as the actual voltage. $bat1-OCV$ is the open circuit voltage signal of the simple model which is fed into the battery model shown in fig. 4.2. The behavior of the terminal estimation voltage y_k and actual voltage is shown in fig. 5.12. It is clearly shown that terminal voltage almost achieves the same level as actual voltage. The first phase of both voltages is due to discharges spike by SOC, and second phase is due to the charges spike. The simple model performs well. Similarly SOC, charging and discharging current and Battery power is shown in figs.5.13, 5.14 and 5.15 for the simple model respectively.

6.2 The Combined model

In fig. 5.17, behavior of ”yk” terminal estimation voltage which is the required goal of the model to achieve it as same as the actual voltage. The combined model slightly under perform as there are some steady state errors showing in the fig. 5.17. By comparing fig. 5.12 of the simple model and fig. 5.17 of the combined model for the terminal estimation voltage and actual voltage, the simple model perform better in estimating the exact the terminal voltage as value of the actual voltage. Fig. 5.18 shows the SOC behavior, figs. 5.19 and 5.20 shows the battery power and charging and discharging current of the battery. The positive line in the figure shows the charging status while the negative lines shows the discharging behaviour of the battery.

6.3 The Hysteresis model

Fig. 5.22 shows the comparison of actual voltage and estimated terminal voltage. It is cleared that zero state hysteresis achieved remarkably this level. It is noted that value of actual voltage and terminal estimated voltage is 4.2. In graph, analysis for pack battery cells i.e 86.
Fig. 5.23 shows the SOC behavior, figs. 5.24 and 5.25 shows the battery power and charging and discharging current of the battery. Again, the positive line in the figure shows the charging status while the negative lines shows the discharging behaviour of the battery.

6.4 Comparison between Simple,Combined and Zero-hysteresis models

By closely monitoring the behaviour of all proposed cell models for terminal estimated voltage of the battery; figs. 5.12, 5.17 and 5.22. The results are more effective with the zero state hysteresis model as compared to the other proposed cell models having no disturbance or steady state error in achieving the same level with actual voltage. Other cells model such as the combined model, does show some steady state error, disturbance and spike of terminal estimation voltage over actual voltage. The simple model does good job in maintaining the level of the both voltages at almost at the same level. However, this models they lack in estimating the steady-state period.

6.5 The Thevenin model

New simulation has been done for this case by considering all the proposed mathematical cell models for observing the terminal voltage estimation with actual voltage: The simple model, The combined model and the zero state hysteresis model. All these three models have been tested by implementing them in the Thevenin circuit model. The new simulink block for the thevenin circuit BMS is shown in fig. 5.26.The new added RC branch is shown in the new equivalent circuit. This added part of the circuit allows to estimate the diffusion voltages such as the Warburg impedance, in the steady-state period. Fig. 5.27 shows the comparison of terminal estimation voltage with actual voltage for all the proposed models. It is clearly shown the performance of the zero state hysteresis model outclass the other models in term of thevenin circuit battery too.

Chapter 7

Environmental Impact

Professor Gregory Plett suggested a simple calculation taking into account some assumption to investigate if lithium material is going to run out due to the surge in demand of electrical vehicles [28]. Talking about fossil fuels, we are using fossil fuel to supply the energy demand. Due to the fact that our planet does not have enough oil source to meet the future energy demand, the question risen by the Professor is if we are going to make up for the oil crisis with a lithium one.

Let us consider the case we are going to adopt lithium-ion batteries cells for large scale applications, like electric vehicles and grid storage and so on, are we going to consume lithium at such a high rate that we are likely to run out of lithium very soon? People are pointing out this potential issue.[28]. The chart is from United States Geological Survey [29] and shows the relative abundance of every element in the periodic table in the earth's crust. As it is shown in the table, the elements are listed by their atomic number on the x-axis and by their relative abundance on the y-axis. The latter one is shown according to a logarithmic scale. Having a look at lithium material, it results between 20 and 100 times more abundant than either lead or nickel, which are commonly used in the battery nowadays.

So, at first sight it looks like that there could be more than enough resource of lithium for batteries, at least compared to lead acid and nickel-based chemistries. One important consideration is that being lithium one of the most reactive elements, is quite difficult to find deposits in nature. In addition, lithium is usually found in some lithium-based compound and not isolated in its elemental form, all by itself. Thus, we must take into account that the lithium found in nature needs a further process in order to be extracted.

The most common ways of obtaining it in nature is from enormous piles of lithium salt flats, usually in South America, but they can be found also in other places, contain high quantities of these lithium-based salt compounds. So lithium is obtained by mining these salt flats, by taking these salts and processing them, and then extracting the lithium from them. It is noticeable how the relative abundance of cadmium and mercury, whose usage is deprecated because of their toxicity, are about 1000 times less common

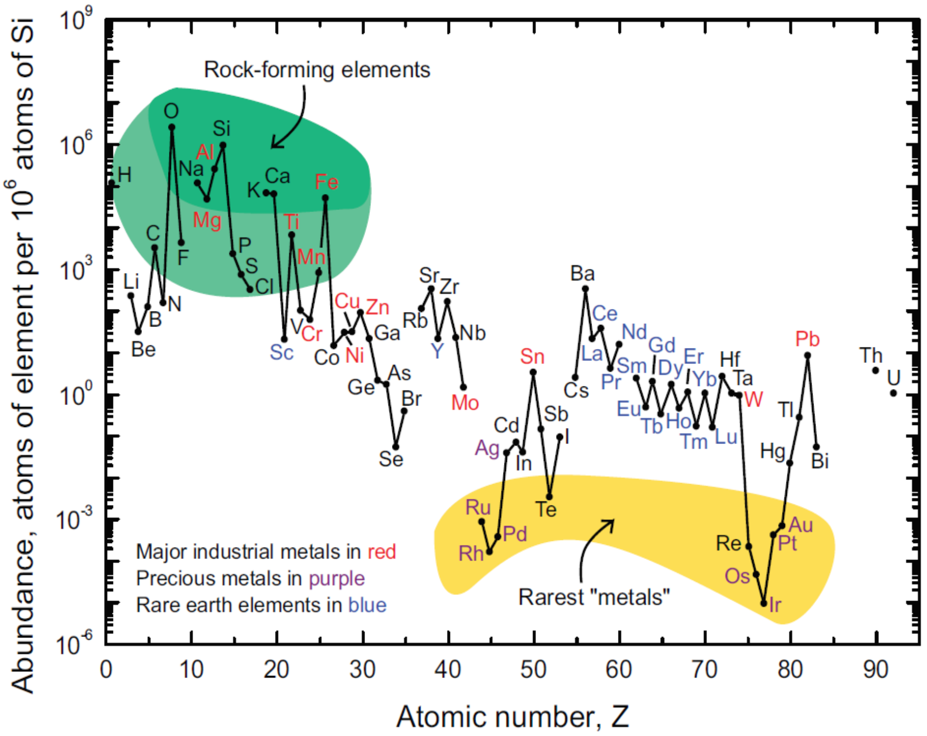

Figure 7.1: lithium availability [29]

than lithium, but they're still used commercially including in battery cells.

Lithium is relatively abundant on this planet; our concern is the amount of it related to the electric car. For purpose of example, we consider a lithium cobalt oxide battery cell. By calculating the mean atomic weight of lithium cobalt oxide, we can find that the lithium content is about 7 percent by weight of the total. This considering just the positive electrodes that is just one-third of the cell weight. So, one-third of the seven percent results to be two percent of the cell weight [28]. We have not considered the lithium content in the negative electrode because when the cell is manufactured there is no lithium in the negative electrode. So, when the battery is charged for the first time the lithium enters the negative electrode. This is the reason why we are considering only how much lithium is in a fresh lithium cobalt oxide electrode.

The salt used in the electrolyte LiPF6 also contains lithium which is the 10 percent of the total electrolyte. The electrolyte as well is just the 10 percent of the total cell weight, so considering the 10 percent of the 10 percent, the lithium accounts for just 1 percent of the cell weight.The total amount of lithium is less than 3 percent in a high-energy battery cell, considering its content in the lithium cobalt oxide and electrolyte.

According to G.Plett batteries that are mostly utilized in hybrid and electric vehicles have a weight of seven kilogram every kilowatt hour. So, considering the three percent lithium content before calculated we can easily find that our lithium content is of 0.2 [28] kilograms per kilowatt hour. Now we take as

Assumptions	Value
Battery cell considered	LCO
Positive electrode considered	$LiCoO_2$
Lithium content by weight in the electrode	7%
Electrolyte content in % by weight in the cell	10%
Total lithium content in high-energy cell by weight	$\leq 3\%$
xEV Cell weight	$7kg/kWh$
Li Content of xEv	$0.2kg/kWh$
Electric car range	$200miles$
Battery Capacity needed	$60kWh$
Lithium per vehicle	$12Kg$
Vehicles assumed	$1million$
Lithium needed worldwide	$12000tons$
Lithium needed considering PHEV	$1200tons$
Lithium on the planet	$200billiontons$
Car per person worldwide	$2000car/person$
Recycling	NO

Table 7.1: Assumptions Environmental Impact [28]

example a Nissan Leaf [30] with an electric range of 200 miles and a battery pack with a capacity of 60-kilowatt hour as an extreme case, because a plug-in hybrid vehicle utilizes much less electric range. Considering the lithium content just calculated we obtain 12 kilograms of lithium per electric car [28].. Considering 1 million electric cars with 12 kilograms of lithium for a car, we obtain 12,000 tons of lithium. A plug-in electric car has a 10 percent of this lithium content.

This would mean 2000 electric car for every person in this world. It is a striking amount. Comparing 12,000 tons of lithium with the 200 billion tons availability worldwide [28]. The professor made an optimistic calculation because the major lithium availability of lithium is found in the seawater which is quite difficult to extract. Nevertheless, every year new lithium deposit has being finding and what is important to mention is that this calculation does not include the recycling part, so of course is difficult to go towards a lithium crisis.

On the other hand, there are other elements used in the Lithium battery that have a more complex situation. Talking about the negative electrodes, this one is usually made up of graphite which means carbon. Carbon fortunately is largely available worldwide. However, for the positive electrode, Cobalt is the most used as material. Unfortunately, there some issues about it: first of all this element is quite rare and is mostly founded in the Republic of Congo; secondly this region is affected by political instability; lastly miners in charge of extracting the material are exposed to serious health problem risking their lives most of the time. So this element is what we need to point out as rare material for battery manufacturing. Luckily, there are many other materials are being explored that can overcome this difficulty such as NMC, NCA and LMO. These elements can drastically lower the amount of Cobalt used.

To sum up, we have seen as Lithium and carbon are not affected by a possible crisis. However, Cobalt has serious issues to be addresses as rare material, political context and health life risk of the miners involved in extracting it. There are many other materials being used in order to substitute this material. One last positive point is that this rough calculation did not take into account the case of recycling the materials that makes an overall better scenario.

Chapter 8

Project Budget and Battery market

This chapter will address the cost of the battery pack and have a look at the battery back market.

8.1 Battery cost

According to the sizing made in the chapter of Data inputs we have INR 18650-20R Battery with a cell capacity equal to 2000mAh.The battery pack is made up by 86 cells in series and 44 cells. The cost of one cell is 14,58 € [31].

$$TotalBatterypackcost = Costonecell * (Ncells_{series} + Ncells_{parallel}) \tag{8.1}$$

Tolal battery pack cost is 1895.46 €. The company manufacturing is Samsung.

8.2 Project Cost

In this section of the Project Budget, the author gives the total estimation of the project's cost. The main costs considered for the realization of this thesis are the following:

- hourly working costs
- material costs

The hourly costs are been funded by the Erasmus Traineeship. The student has been payed the amount $8/h$ for a the total of $500h$. About the material cost, the student has been in charged of buying a new laptop (HP Pavilion x360 Convertible 14-cd0xxx) that could support the working power to manage such simulation in MATLAB/Simulink environment.

The following equation show the total hourly working cost and the final costs:

$$Hourly_{costs} = Total_{Hours} * Student_{salary} = 500h * 8/h = 4000; \tag{8.2}$$

$$TOTAL_{costs} = Hourly_{costs} + Material_{costs} = 4000 + 750 = 4750 \tag{8.3}$$

All the other costs were not relevant or not purchased by the UPC university, nor by the Erasmus Program.

8.3 Project Management

The whole project has been divide by the author in two periods : First Period Project in Fig. 8.1, and Second Period Project in Fig. 8.2.

In the First Period Project the author completed the following tasks:

- Choice of the Project
- Own literature research
- Start to model the battery
- Dc-Dc Converter Modeling

In the Second Period Project the author completed the following tasks:

- Find parameters for the battery models
- Issues in battery modelling
- Further study of Data Algorithms, course Gregory Plett.
- Thevenin Modeling
- Comparison Models

8.4 Battery Market

Over the last decade the lithium-ion battery has been dropping its market value. The report of Bloomberg New Energy [1] explains why this happened and forecasted interesting trend for the future. In Particular in Fig. 8.3 shows how the annual-ion battery price lowered its valued by approximately 20% each year. $1000\ \$/kWh$ was the price for lithium-ion in year 2010, $273\ \$/kWh$ in the 2016.

This steep decrease in prices from year 2017 to year 2030, BNEF in the previous years was partially possible in virtue of the technology improvements and economies. Nevertheless the severe competition between the major manufacturers has been vital in dropping the prices.

[1] estimate the future annual lithium-ion battery prices towards 2030. The model was implemented taking into account a cost production of a Korean manufacturing plant. These are the assumptions:

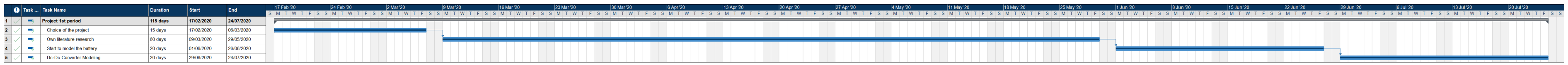

Figure 8.1: Project 1st period

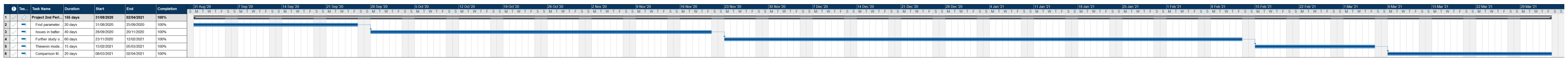

Figure 8.2: Project 2nd period

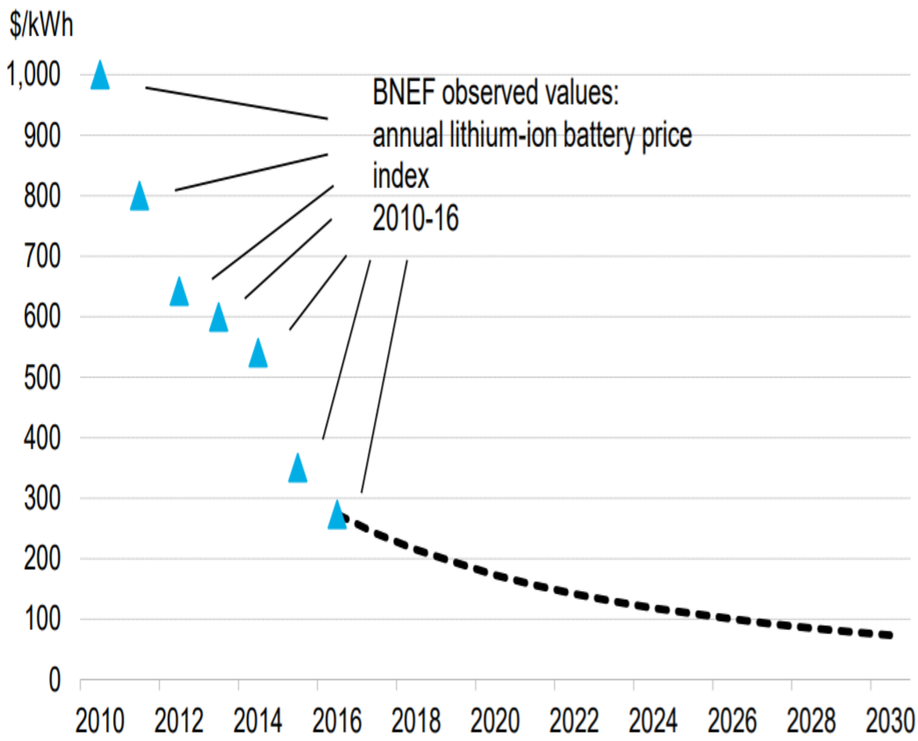

Figure 8.3: Forecasted lithium-ion battery pack price [1]

- Reduction of production cost, Improved processes and development of new chemestries due the fierce competition among the leading manufacturers;
- Increase in sell of EV;

In particular the price will reach a value of $73\ \$/kWh$ in year 2030.

In Fig. 8.4 is shown a forecasted electric car demand from year 2010 to year 2030. The chart shows a rapid growing demand in EV sales with a total of $408\ GWh$ in year 2025 and $1293\ GWh$ in year 2030. China is seen as the main rise in EV Demand sales, generating a sort of separator supply bottleneck [1]. The report [1] also shows a growth in stationary-storage market from $65\ GWh$ in year 2025 and $200\ GWh$ in year 2030.

Along with the EV sale growth demand, the report forecasts also a decrease in EV prices. In Fig. 8.5 depicts the price drop of EVs depending on its price components. Battery components accounts for the 48% of total EV price in 2016, 27% in 2024 and 18% in 2030. The charts also compares the total cost EV with the Internal combustion engine vehicle average price. ICE is almost constant at 30 thousand dollars along the period considered with a slight rise by year 2030. EV price starts in 2016 with 44 thousand dollars winning the gap with ICE in year with 28 thousand dollars and still lowering in the next future.

This last chart Fig.8.5 showed how Electric Vehicles will start to be more affordable in the future. This is due to technology developments, the increase EV demand and the fierce competition of the related

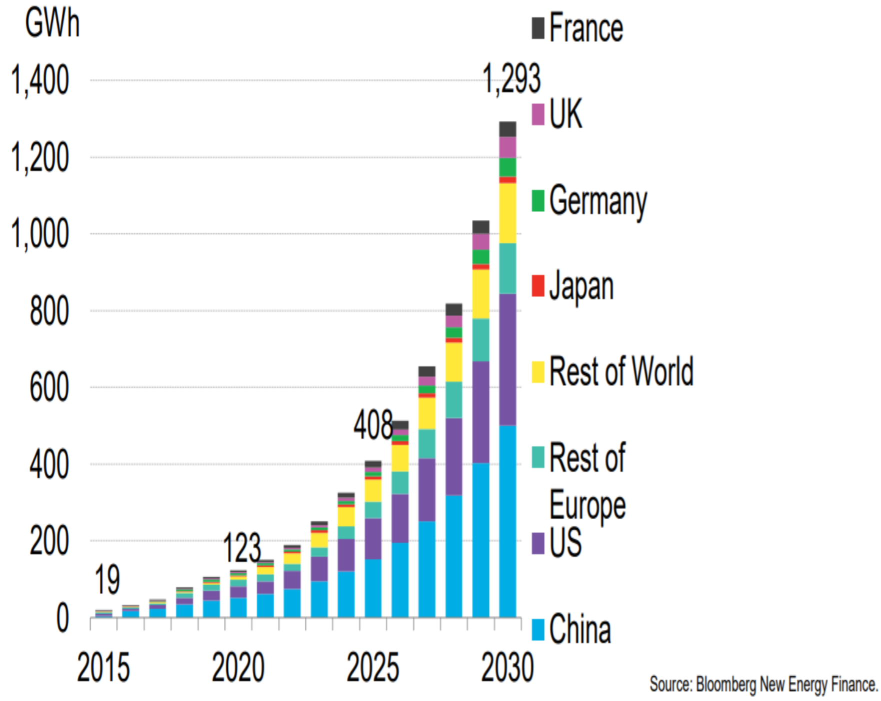

Figure 8.4: Forecasted demand electric cars[1]

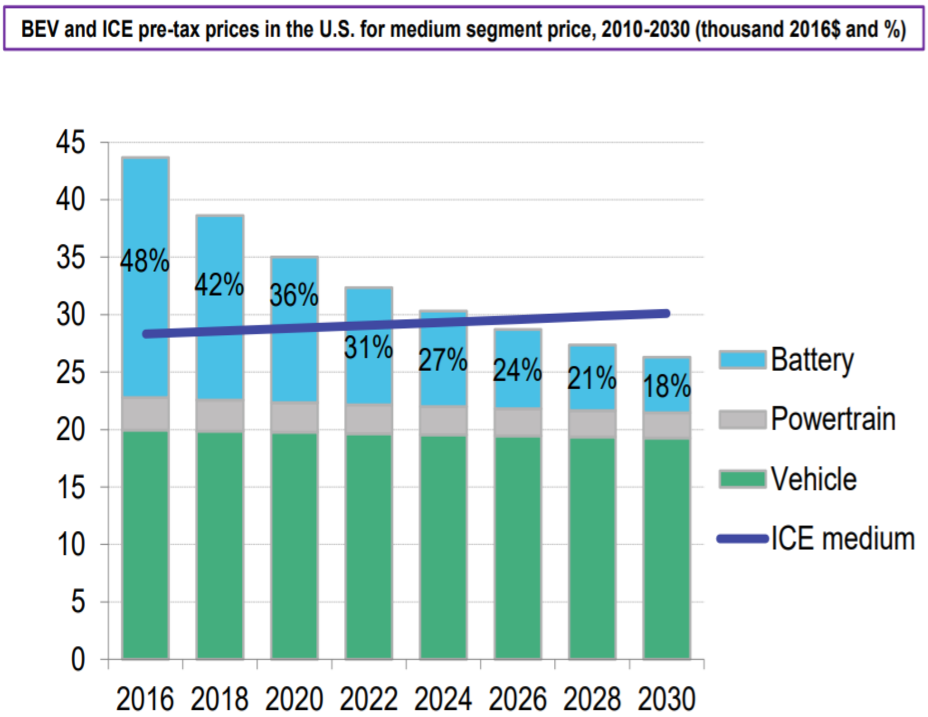

Figure 8.5: BEV forecast price with its components'impacts on the total price. Price compared with the average ICE price[1]

industries.

Bloomberg New Energy Finance points out how the already existing facilities are capable of meeting the future batteries demand. Two major companies are explored and strategies are suggested in order to overcoming this possible issue.

For the Battery manufacturer is advisable to lower the battery cost improving production and research and development of new technologies so that investor would be more captivated by this industry. Another suggestion is to rise their market shares in the stationary storage markets.

For Car company the strategy would be to reduce batteries cost in order to lower the total vehicle price. The way to do that is to sign large long-term contracts with suppliers. Also there is the big opportunity to exploit the second-life battery market by purposing the use of Used batteries. Another idea is to start to produce their own batteries.

Chapter 9

Conclusions

This report has proposed three mathematical cells structure for the purpose of modeling Li-NMC HEV cell dynamics for their eventual role in HEV BMS algorithms. Three different models for cell to estimate terminal voltage have been implemented in MATLAB/Simulink environment. Results are presented to demonstrate the terminal estimation voltage as close to actual voltage and SOC estimation for all the proposed cell models. Single-state model are very simple, perform up to expectation level. The combined cell model performs slightly below than simple model.

In addition, the three models proposed would be better if implemented in a BMS for portable device pack where there is no need of big investment for the battery pack. Indeed, as shown in chapter 4 except for the zero-hysteresis model, the models cannot estimate well the steady-state period when the battery is allowed to rest. This is can be a huge issue for EV application where SOC is a paramount parameter for further estimate Energy, power available and the remaining life of the battery pack.

On other hand, the Thevenin electric circuit fig. 4.3 is a good model especially if combined with the zero-hysteresis model. Indeed, it can estimate quite well all the dynamics of the battery voltage. This helps the BMS to better estimate the parameters, calculate the remaining life of the battery and balance the single cells need . To be crystal clear, in this context the BMS work better. Unfortunately, when we start to implement more sophisticated Algorithms in the BMS the investment cost starts to rise. This is the case of EV environment. In fact, the EV has a huge investment cost of battery and the better way to prolong of the battery is to invest in a optimal BMS.

Investing in excellent BMS can reduce the investment in batteries as well. Indeed, if the Battery Management Systems works pretty well the battery pack may need less battery cells to meet the energy and power demand. This has a remarkable impact also on the design of the Car itself, having more space to place the other components.
Furthermore, there will be needed less maintenance work.

If we want to further optimize the algorithms, we could add hysteresis and filter states to the model aids performance, at some cost in complexity. Another option would be to add other RC branches to the Thevenin Circuit 4.3 to better predict the dynamics of the system and the voltage diffusion.

Finally, this report explored the environmental impact on Lithium sources due to a future growth in demand of EV sales showed and predicted by [1]. The future of lithium is not compromised in virtue of its huge availability. Still, further research is needed to find new technologies that make battery as high sustainable as possible. The surge in EV demand can causes significant and severe consequences such as generating more used batteries. The process and the market of secondary battery life must be strengthened and exploited to help to reuse them.

Bibliography

[1] C. Curry. Lithium-ion battery costs and market. *Bloomberg New Energy Finance*, 5:4–6, 2017.

[2] F. Zheng, Y. Xing, J. Jiang, B. Sun, J. Kim, and M. Pecht. Influence of different open circuit voltage tests on state of charge online estimation for lithium-ion batteries. *Applied energy*, 183:513–525, 2016.

[3] C. Barbier, B. Nogarede, H. Meyer, and S. Bensaoud. A battery state of charge indicator for electric vehicle. In *INSTITUTION OF MECHANICAL ENGINEERS CONFERENCE PUBLICATIONS*, volume 5, pages 29–29. MEDICAL ENGINEERING PUBLICATIONS LTD, 1994.

[4] P. Lürkens and W. Steffens. Ladezustandsschätzung von bleibatterien mit hilfe des kalman-filters. *ETZ-Archiv*, 8(7):231–236, 1986.

[5] D. O. H. J. S. U. H. A. A. L. S. Javier Muñoz Alvarez, Martin Sachenbacher. D6.1 – analysis of the state of the art on bms, 2017.

[6] D. Andrea. *Battery management systems for large lithium-ion battery packs*. Artech house, 2010.

[7] G. L. Plett. *Battery management systems, Volume II: Equivalent-circuit methods*. Artech House, 2015.

[8] M. Jung and S. Schwunk. High end battery management systems for renewable energy and ev applications. *Green*, 3(1):19–26, 2013.

[9] G. L. Plett. *Battery management systems, Volume I: Battery modeling*. Artech House, 2015.

[10] S. Piller, M. Perrin, and A. Jossen. Methods for state-of-charge determination and their applications. *Journal of power sources*, 96(1):113–120, 2001.

[11] W. Gu and C. Wang. Thermal-electrochemical modeling of battery systems. *Journal of The Electrochemical Society*, 147(8):2910, 2000.

[12] E. Barsoukov, J. H. Kim, C. O. Yoon, and H. Lee. Universal battery parameterization to yield a non-linear equivalent circuit valid for battery simulation at arbitrary load. *Journal of power sources*, 83(1-2):61–70, 1999.

[13] S. Rodrigues, N. Munichandraiah, and A. Shukla. A review of state-of-charge indication of batteries by means of ac impedance measurements. *Journal of power Sources*, 87(1-2):12–20, 2000.

[14] A. J. Salkind, C. Fennie, P. Singh, T. Atwater, and D. E. Reisner. Determination of state-of-charge and state-of-health of batteries by fuzzy logic methodology. *Journal of Power sources*, 80(1-2): 293–300, 1999.

[15] P. Singh, C. Fennie, D. Reisner, and A. Salkind. Fuzzy logic-enhanced electrochemical impedance spectroscopy (fleeis) to determine battery state-of-charge. In *Fifteenth Annual Battery Conference on Applications and Advances (Cat. No. 00TH8490)*, pages 199–204. IEEE, 2000.

[16] K. Takano, K. Nozaki, Y. Saito, A. Negishi, K. Kato, and Y. Yamaguchi. Simulation study of electrical dynamic characteristics of lithium-ion battery. *Journal of power sources*, 90(2):214–223, 2000.

[17] A. Kawamura and T. Yanagihara. State of charge estimation of sealed lead-acid batteries used for electric vehicles. In *PESC 98 Record. 29th Annual IEEE Power Electronics Specialists Conference (Cat. No. 98CH36196)*, volume 1, pages 583–587. IEEE, 1998.

[18] H. Chan. A new battery model for use with battery energy storage systems and electric vehicles power systems. In *2000 IEEE Power Engineering Society Winter Meeting. Conference Proceedings (Cat. No. 00CH37077)*, volume 1, pages 470–475. IEEE, 2000.

[19] V. H. Johnson, A. A. Pesaran, and T. Sack. Temperature-dependent battery models for high-power lithium-ion batteries. Technical report, National Renewable Energy Lab., Golden, CO (US), 2001.

[20] R. Giglioli, P. Pelacchi, M. Raugi, and G. Zini. A state of charge observer for lead-acid batteries. *Energ. Elettr.;(Italy)*, 55(1), 1988.

[21] G. Plett. Lipb dynamic cell models for kalman-filter soc estimation. In *The 19th international battery, hybrid and fuel electric vehicle symposium and exhibition*, pages 1–12. Citeseer, 2002.

[22] T. Inc. Battery modeling for hev simulation by thermoanalytics inc. URL `https://www.thermoanalytics.com/support/publications/batterymodelsdoc.html`.

[23] G. L. Plett. Extended kalman filtering for battery management systems of lipb-based hev battery packs: Part 2. modeling and identification. *Journal of power sources*, 134(2):262–276, 2004.

[24] V. Srinivasan, J. W. Weidner, and J. Newman. Hysteresis during cycling of nickel hydroxide active material. *Journal of the Electrochemical Society*, 148(9):A969, 2001.

[25] S. Susanna, B. R. Dewangga, O. Wahyungoro, and A. I. Cahyadi. Comparison of simple battery model and thevenin battery model for soc estimation based on ocv method. In *2019 International Conference on Information and Communications Technology (ICOIACT)*, pages 738–743. IEEE, 2019.

[26] G.L.Plett. What is hysteresis in a lithium-ion cell and how can i model it?, . URL `https://www.coursera.org/lecture/equivalent-circuit-cell-model-simulation/2-1-7-what-is-hysteresis-in-a-lithium-ion-cell-and-how-can-i-model-it-Uocsg`.

[27] F. Díaz-González, A. Sumper, and O. Gomis-Bellmunt. *Energy storage in power systems*. John Wiley & Sons, 2016.

[28] G.L.Plett. Is lithium going to run out?, . URL https://www.coursera.org/learn/battery-management-systems/supplement/N1F8J/notes-for-lesson-1-2-6.

[29] S. B. By Gordon B. Haxel and S. M. from USGS. United states geological survey. rare earth elements—critical resources for high technology. URL http://pubs.usgs.gov/fs/2002/fs087-02/.

[30] B. H. from GREEN CAR REPORTS. Nissan's 60-kwh, 200-mile battery pack: What we know so far. URL https://www.greencarreports.com/news/1100775_nissans-60-kwh-200-mile-battery-pack-what-we-know-so-far.

[31] rs online. Pila recargable 18650 de ión-litio, 3.6v, 2ah, terminal plano, samsung. URL https://es.rs-online.com/web/p/baterias-recargables-de-tamanos-especiales/8182992/.

Appendix A

Technical Datasheets

It is possible to add PDF files to the document, such as technical sheets of some equipment used in the work.

A.1 Battery Datasheet

Spec. No.	INR18650-20R	Version No.	1.2	In-Young Jang

SPECIFICATION OF PRODUCT

Lithium-ion rechargeable cell for power tools

Model name : INR18650-20R

Dec., 2011

Samsung SDI Co., Ltd.

Energy Business Division

Spec. No.	INR18650-20R	Version No.	1.2	In-Young Jang

Contents

1.0. Scope

This product specification has been prepared to specify the rechargeable lithium-ion cell ('cell') to be supplied to the customer by Samsung SDI Co., Ltd.

2.0. Description and model

2.1 Description lithium-ion rechargeable cell

2.2 Model name INR18650-20R

3.0. Nominal specifications

Item	**Specification**
3.1 Nominal discharge capacity	2,000mAh Charge: 1A, 4.20V,CCCV 100mA cut-off, Discharge: 0.2C, 2.5V discharge cut-off
3.2 Nominal voltage	3.6V
3.3 Standard charge	CCCV, 1A, 4.20 ± 0.05 V, 100mA cut-off
3.4 Rapid charge	CCCV, 4A, 4.20 ± 0.05 V, 100mA cut-off
3.6 Charging time	Standard charge : 180min / 100mA cut-off Rapid charge: 50min (at 25℃) / 100mA cut-off
3.7 Max. continuous discharge (Continuous)	22A(at 25℃), 60% at 250 cycle
3.8 Discharge cut-off voltage End of discharge	2.5V
3.9 Cell weight	45.0g max
3.10 Cell dimension	Height : 64.85 ± 0.15mm Diameter : 18.33 ± 0.07mm
3.11 Operating temperature (surface temperature)	Charge : 0 to 50℃ (recommended recharge release < 45℃) Discharge: -20 to 75℃ (recommended re-discharge release < 60℃)
3.12 Storage temperature (Recovery 90% after storage)	1.5 year -30~25℃(1*) 3 months -30~45℃(1*) 1 month -30~60℃(1*)

Note (1): If the cell is kept as ex-factory status (50±5% SOC, 25℃), the capacity recovery rate is more than 90% of 10A discharge capacity 100% is1,950mAh at 25℃ with SOC 100% after formation.

4.0 Outline dimensions

See the attachment (Fig. 1)

5.0. Appearance

There shall be no such defects as scratch, rust, discoloration, leakage which may adversely affect commercial value of the cell.

6.0. Standard test conditions

6.1 Environmental conditions

Unless otherwise specified, all tests stated in this specification are conducted at temperature 25±5℃ and humidity 65±20%.

6.2 Measuring equipment

(1) Amp-meter and volt-meter

The amp-meter and volt-meter should have an accuracy of the grade 0.5mA and mV or higher.

(2) Slide caliper

The slide caliper should have 0.01 mm scale.

(3) Impedance meter

The impedance meter with AC 1kHz should be used.

7.0. Characteristics

7.1 Standard charge

This "Standard charge" means charging the cell CCCV with charge current 0.5CmA (1,000mA), constant voltage 4.2V and 100mA cut-off in CV mode at 25℃ for capacity. .

7.2 Rapid charge

Rapid charge means charging the cell CCCV with charge current 4A and 100mA cut-off at 25℃

7.3 Nominal discharge capacity

The standard discharge capacity is the initial discharge capacity of the cell, which is measured with discharge current of 400mA(0.2C) with 2.5V cut-off at 25℃ within 1hour after the standard charge.

Nominal discharge capacity ≥ 2,000mAh

Which complying to the minimum capacity of IEC61960 standard.

7.4 Standard rated discharge capacity

The standard rated discharge is the discharge capacity of the cell, which is measured with discharge current of 10A with 2.5V cut-off at 25℃ within 1hour after the standard charge.

Standard rated discharge capacity ≥ 1,950mAh

7.5 Initial internal impedance

Initial internal impedance measured at AC 1kHz after standard charge

Initial internal impedance ≤ 18mΩ

7.6 Temperature dependence of discharge capacity

Capacity comparison at each temperature, measured with discharge constant current 10A and 2.5V cut-off after the standard charge is as follows.

Discharge temperature				
-20℃	-10℃	0℃	25℃	60℃

60%	75%	80%	100%	100%

Note: If charge temperature and discharge temperature is not the same,
the interval for temperature change is 3 hours.
Percentage index of the discharge at 25℃ at 10A (=1,950mAh) is 100%.

7.7 Temperature dependence of charge capacity

Capacity comparison at each temperature, measured with discharge constant current 10A and 2.5V cut-off after the standard charge is as follows.

	Charge temperature					Discharge temperature
	0℃	5℃	25℃	45℃	50℃	25℃
Relative capacity	80%	90%	100%	95%	95%	

Note: If charge temperature and discharge temperature is not the same,
the interval for temperature change is 3 hours.
Percentage index of the discharge at 25℃ at 10A (=1,950mAh) is 100%.

7.8 Charge rate capabilities

Discharge capacity is measured with constant current 10A and 2.5V cut-off after the cell is charged with 4.2V as follows.

	Charge condition	
Current	Standard 1A	Maximum rapid charge 4A
Cut-off	100mA	100mA
Relative Capacity	100%	98%

Note: Percentage index of the discharge at 25℃ at 10A (=1,950mAh) is 100%.

7.9 Discharge rate capabilities

Discharge capacity is measured with the various currents in under table and 2.5V cut-off after the standard charge.

	Discharge condition				
Current	0.40A	4A	10A	18A	20A
Relative Capacity	100%	97%	100%	97%	95%

Percentage index of the discharge at 25℃ at 10A (=1,950mAh) is 100%.

7.10 Cycle life

With standard charge and maximum continuous discharge.
Capacity after 250cycles,

Capacity ≥ 1,200mAh (60% of the nominal capacity at 25℃)

7.11 Storage characteristics

Standard rated discharge capacity after storage for 1 month at 60℃ from the standard charged state is ≥ 90% of the initial 10A discharge capacity at 25℃

7.12 Status of the cell as of ex-factory

The cell should be shipped in 50 ± 5% charged state. In this case, OCV is from 3.600V to 3.690V.

8.0. Mechanical Characteristics

8.1 Drop test

Test method: Cell(as of shipment or full charged) drop onto the oak-board (thickness: ≥30mm) from 1.0m height at a random direction 6 times.

Criteria: No leakage, Voltage decrease≦0.025V, AC iR increase ≦1.0mΩ

8.2 Vibration test

Test method: As to the UN transportation regulation(UN38.3), for each axis (X and Y axis with cylindrical cells) 7Hz→200Hz→7Hz for 15min, repetition 12 times totally 3hours, the acceleration 1g during 7 to 18Hz and 8g (amplitude 1.6mm) up to 200Hz.

Criteria: No leakage, with less than 10mV of OCV drop

9.0. Safety

9.1 Overcharge test

Test method: To charge with 20A-20V at 25℃ for 2hr.

Criteria: No fire, and no explosion.

9.2 External short-circuit test

Test method: To short-circuit the standard charged cell (or 50% discharged cell) by connecting positive and negative terminal by 50mΩ wire for 10min.

Criteria: No fire, and no explosion.

9.3 Reverse charge test

Test method: To charge the standard charged cell with charge current 10A By 0V for 2.5 hours.

Criteria: No fire, and no explosion.

9.4 Heating test

Test method: To heat up the standard charged cell at heating rate 5℃ per minute up to 150℃ and keep the cell in oven for 10 minutes.

Criteria: No fire, and no explosion.

10.0. Warranty

Samsung SDI will be responsible for replacing the cell against defects or poor workmanship for 18months from the date of shipping. Any other problem caused by malfunction of the equipment or mix-use of the cell is not under this warranty.

The warranty set forth in proper using and handling conditions described above and excludes in the case of a defect which is not related to manufacturing of the cell.

11.0. Others

11.1 Storage for a long time

If the cell is kept for a long time (3 months or more), It is strongly recommended that the cell is preserved at dry and low-temperature.

11.2 Others

Any matters that specifications do not have, should be conferred with between the both parties.

12.0. Packing

See Fig.2,

Package Drawing

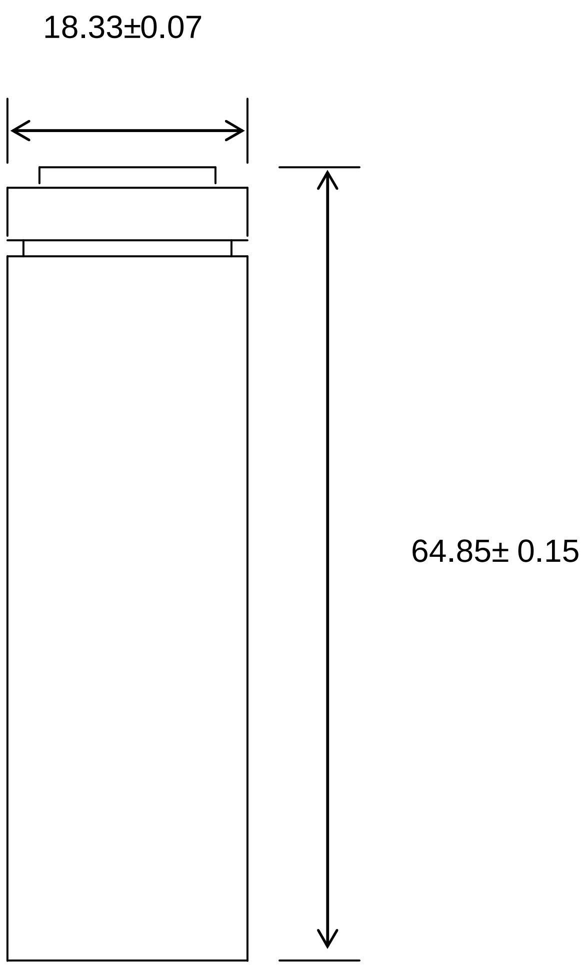

Unit : mm
With tube

Fig.1. Outline dimensions of INR110500-20R

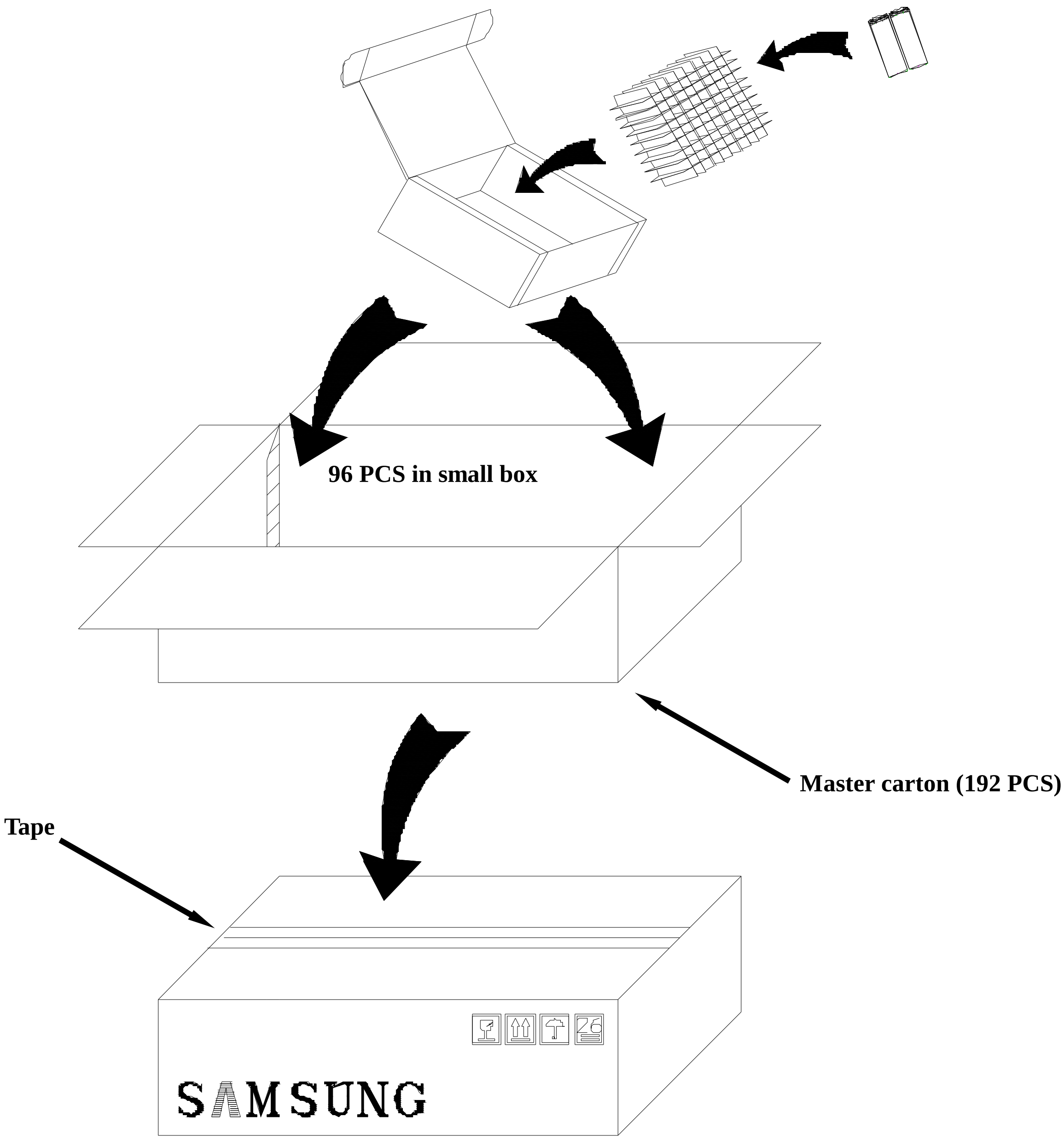

Fig.2. Package drawing

Proper use and handling of lithium ion cells

See before using lithium-ion cell
Supplied by
Samsung SDI Co., Ltd.

1.0. General

This document has been prepared to describe the appropriate cautions and prohibitions, which the customer should take or employ when the customer uses and handles the lithium ion cell to be manufactured and supplied by Samsung SDI Co., Ltd., in order to obtain optimal performance and safety.

2.0. Charging

2.1 Charging current

Charging current shall be less than maximum charge current specified in the product specification.

2.2 Charging voltage

Charging shall be done by voltage less than that specified in the product specification.

2.3 Charging time

Continuous charging under specified voltage does not cause any loss of performance characteristics. However, the charge timer is recommended to be installed from a safety consideration, which shuts off further charging at time specified in the product specification.

2.4 Charging temperature

The cell shall be charged within a range of specified temperatures in the specification.

2.5 Reverse charging

The cell shall be connected, confirming that its poles are correctly aligned.
Inverse charging shall be strictly prohibited. If the cell is connected improperly, it may be damaged.

3.0. Discharging

3.1 Discharging

3.1.1 The cell shall be discharged continuously at less than maximum discharge current specified in the product specification. In case of the higher discharge current should be set, it shall be discussed together with SDI.

3.2 Discharging temperature

3.2.1 The cell shall be discharged within a range of temperatures specified in the product specification.

3.2.2 Otherwise, it may cause loss of performance characteristics.

3.3 Over-discharging

3.3.1 The system should equip with a device to prevent further discharging exceeding discharging cut-off voltage specified in the product specification.

3.3.2 Over-discharging may cause loss of performance characteristics of battery.

3.3.3 Over-discharging may occur by self-discharge if the battery is left for a very long time without any use.

3.3.4 The charger should equip with a device to detect voltage of cell block and to determine recharging procedures.

4.0. Storage

4.1 Storage conditions

4.1.1 The cell should be stored within a range of temperatures specified in the product specification.

4.1.2 Otherwise, it may cause loss of performance characteristics, leakage and/or rust.

4.2 Long-term storage

4.2.1 The cell should be used within a short period after charging because long-term storage may cause loss of capacity by self-discharging.

4.2.2. If long-term storage is necessary, the cell should be stored at lower voltage within a range specified in the product specification, because storage with higher voltage may cause more loss of performance characteristics.

5.0. Cycle life

5.1 Cycle life performance

5.1.1 The cell can be charged/discharged repeatedly up to times specified in the product specification with a certain level of capacity specified in the product specification.

5.1.2 Cycle life may be determined by conditions of charging, discharging, operating temperature and/or storage.

6.0. Design of system

6.1 Connection between the cell and the battery

6.1.1 The cell should not be soldered directly with other cells. Namely, the cell should be welded with leads on its terminal and then be soldered with wire or leads to solder.

6.1.2 Otherwise, it may cause damage of component, such as separator and insulator, by heat generation.

6.2 Positioning the battery in the system

6.2.1 The battery should be positioned as possible as far from heat sources and high temperature components.

6.2.2 Otherwise, it may cause loss of characteristics.

6.2.3 The recommended spacing between the cells is more than 1mm.

6.3 Mechanical shock protection of the battery

6.3.1 The battery should be equipped with appropriate shock absorbers in the pack in order to minimize shock, which can damage the cells.

6.3.2 Otherwise, it may cause shape distortion, leakage, heat generation and/or rupture and/or open circuit.

6.4 Short-circuit protection of the cell

6.4.1 The cell equips with an insulating sleeve to protect short-circuit which may occur during transportation, battery assembly and /or system operation.

6.4.2 If the cell sleeve is damaged by some cause such as outside impact, it may cause short-circuit with some wiring inside the battery.

6.5 Connection between the battery and charger/system

6.5.1 The battery should be designed to be connected only to the specified charger and system.

6.5.2 A reverse connection of the battery, even in the specified system, should be avoided by employing special battery design such as a special terminals.

6.6 Pack design

6.6.1 The current consumption of the battery pack should be under 10uA at sleep mode.

6.6.2 Cell voltage monitoring system.
The system (charger or pack) should be equipped with a device to monitor each

voltage of cell block to avoid cell imbalance which can cause damage to the cells.

6.6.4 The battery pack or system should have warning system such as over temperature, over voltage, over current, and so on.

7.0. Battery pack assembly

7.1 Prohibition of usage of damaged cell

7.1.1 The cell should be inspected visually before battery assembly.

7.1.2 The cell should not be used if sleeve-damage, can-distorsion and/or electrolyte-smell is detected.

7.2 Terminals handling

7.2.1 Excessive force on the negative terminal should be avoided when external strip terminal is welled.

7.3 Transportation

7.3.1 If the cell is necessary to be transported to such as the battery manufacturer, careful precautions should be taken to avoid damage of cell.

8.0. Others

8.1 Disassembly

8.1.1 The cell should not be dismantled from the battery pack.

8.1.2 Internal short-circuit caused by disassembly may lead to heat generation and/or venting.

8.1.3 When the electrolyte is coming in contact with the skin or eyes, flush immediately with fresh water and seek medical advice.

8.2 Short-circuiting

8.2.1 Short-circuit results in very high current which leads to heat generation.

8.2.3 An appropriate circuitry should be employed to protect accidental short-circuiting.

8.3 Incineration

8.3.1 Incinerating and disposing of the cell in fire are strictly prohibited, because it may cause rupture and explosion.

8.4 Immersion

8.4.1 Soaking the cell in water is strictly prohibited, because it may cause corrosion and leakage of components to be damaged to functions

8.5 Mixing use

8.5.1 Different types of cell, or same types but different cell manufacturer's shall not be used, which may lead to cell imbalance, cell rupture or damage to system due to the different characteristics of cell.

8.6 Battery exchange

8.6.1 Although the cell contains no environmentally hazardous component, such as lead or cadmium, the battery shall be disposed according to the local regulations when it is disposed.

8.6.2 The cell should be disposed with a discharged state to avoid heat generation by an inadvertent short-circuit.

8.7 Caution

The Battery used in this device may present a risk of fire or chemical burn if mistreated.

Do not disassemble, expose to heat above 100℃ or incinerate it.

Replace battery with those of Samsung SDI only.

Use of another battery may cause a risk of fire or explosion.

Dispose of used battery promptly.

Keep battery away from children.
Do not disassemble and do not dispose of battery in fire.

8.8 Warning – Attached

Handling precaution and prohibitions of lithium Ion rechargeable cells and batteries

Inaccurate handling of lithium ion and lithium ion polymer rechargeable battery may cause leakage, heat, smoke, an explosion, or fire.

This could cause deterioration of performance or failure. Please be sure to follow instructions carefully.

1.1 Storage

Store the battery at low temperature (below 25℃ is recommended), low humidity, no dust and no corrosive gas atmosphere.

1.2 Safety precaution and prohibitions

To assure product safety, describe the following precautions in the instruction manual of the application.

[Danger!]

■ Electrical misusage

Use stipulated charger.

Use or charge the battery only in the stipulated application.

Don't charge the battery by an electric outlet directly or a cigarette lighter charger.

Don't charge the battery reversely.

■ Environmental misusage

Don't leave the battery near the fire or a heated source.

Don't throw the battery into the fire.

Don't leave, charge or use the battery in a car or similar place where inside of temperature may be over 60℃.

Don't immerse, throw, wet the battery in water / sea water.

■ others

Don't fold the battery cased with laminated film such as pouch and polymer.

Don't store the battery in a pocket or a bag together with metallic objects such as keys, necklaces, hairpins, coins, or screws.

Don't short circuit (+) and (-) terminals with metallic object intentionally.

Don't pierce the battery with a sharp object such as a needle, screw drivers.

Don't heat partial area of the battery with heated objects such as soldering iron.

Don't hit with heavy objects such as a hammer, weight.

Don't step on the battery and throw or drop the battery on the hard floor to avoid mechanical shock.

Don't disassemble the battery or modify the battery design including electric circuit.

Don't solder on the battery directly.

Don't use seriously scared or deformed battery.

Don't put the battery into a microwave oven, dryer or high-pressure container.

Don't use or assemble the battery with other makers' batteries, different types and/or models of batteries such as dry batteries, nickel-metal hydride batteries, or nickel-cadmium batteries.

Don't use or assemble old and new batteries together.

[Warning!]

Stop charging the battery if charging isn't completed within the specified time.

Stop using the battery if the battery becomes abnormally hot, order, discoloration, deformation, or abnormal conditions is detected during use, charge, or storage.

Keep away from fire immediately when leakage or foul odors are detected. If liquid leaks onto your skin or cloths, wash well with fresh water immediately.

If liquid leaking from the battery gets into your eyes, don't rub your eyes and wash them with clean water and go to see a doctor immediately.

If the terminals of the battery become dirty, wipe with a dry cloth before using the battery.

The battery can be used within the following temperature ranges. Don't exceed these ranges.

The operating temperature is based on the cell surface temperature in hottest position in pack.

Charge temperature ranges : 0℃ ~ 50℃

Discharge Temperature ranges : -20℃ ~ 75℃

Store the battery at temperature below 60℃

Cover terminals with proper insulating tape before disposal.

[Caution!]

■ Electrical misusage

Battery must be charged with constant current-constant voltage (CC/CV).

Charge current must be controlled by specified value in cell specification.

Cut-off voltage of charging must be less than 4.2 + 0.05V

Charger must stop charging battery by detecting either charging time or current specified in cell's specification.

Discharge current must be controlled by specified value in cell's specification.

Cut-off voltage of full discharging and recharging must be over 2.5V.

■ others

Keep the battery away from babies and children to avoid any accidents such as swallow.

If younger children use the battery, their guardians should explain the proper handling method and precaution before using.

Before using the battery, be sure to read the user's manual and precaution of it's handling.

Before using charger, be sure to read the user's manual of the charger.

Before installing and removing the battery from application, be sure to read user's manual of the application.

Replace the battery when using time of battery becomes much shorter than usual.

Cover terminals with insulating tape before proper disposal.

If the battery is needed to be stored for an long period, battery should be removed from the application and stored in a place where humidity and temperature are low.

While the battery is charged, used and stored, keep it away from object materials with static electric chargers.

Safety handling procedure for the transporter

■ Quarantine

Packages that are crushed, punctured or torn open to reveal contents should not be transported. Such packages should be isolated until the shipper has been consulted, provided instructions and, if appropriate, arranged to have the product inspected and repacked.

■ Spilled product

In the event that damage to packaging results in the release of cells or batteries, the spilled products should be promptly collected and segregated and the shipper should contact for instructions.

Design of positioning the battery pack in application and charger

To prevent the deterioration of the battery performance caused by heat, battery shall be positioned away from the area where heat is generated in the application and the charger.

Design of the battery pack

Be sure adopting proper safe device such as PTC specified type or model in Cell Specification. If you intend to adopt different safety device which is not specified in Cell Specification, please contact Samsung SDI to investigate any potential safety problem.

Be sure designing 2nd protective devices such as PCM at the same time to protect cell just in case one protective device is fault.

Please contact following offices when you need any help including safety concerns.

Samsung SDI emergency contact information

■ **Samsung SDI Cheonan factory CS group**
508, Sungsung-dong, Cheonan-si, Chungnam, Korea
Tel:(+82)70-7125-1806 Fax:(+82)41-560-3697

■ **Samsung SDI America office.**
18600 Broadwick Street Rancho Dominguez CA 90220
Tel:(+1)310-900-5205 Fax:(+1)310-537-1033

■ **Samsung SDI Taiwan office.**
Rm. 3010, 30F., 333, Keelung Rd. Sec. 1, Taipei, Taiwan
Tel:(+886)2-2728-8469 Fax:(+886)2-2728-8480

Additional remarks

■ Cell package : The bare cell is packed by which packaging material, PET tube.

■ Model and tube marking : there are three lines on the cell tube as follows.

Line 1 : INR18650-20R --- cell model name

Line 2 : SAMSUNG SDI --- cell manufacturer

Line 3 : 125 --- part number of 20R

■ Lot marking : There are three lines on the cell metal can as follows.

Line 1 : B0BB --- 1^{st} digit: Line number (“1” for cylindrical line No.1, “B” for cylindrical line No. 4)

2^{nd} digit: Final number of Model Name (“0” is INR18650-20x)

3^{rd} digit: Year (“B” is 2011)

4^{th} digit: Month (“9” is Sep. ; A is Oct., B is Nov., C is Dec)

Line 2 : 7B111 --- 1^{st} digit: Negative coater number (“7” is No. 7 coater)

2^{nd} ~ 4^{th} digit: Batch number

5^{th} digit: Serial No. of assembling

Line 3 : E9 --- 1^{st} digit: Reel No (“E” is E reel ; A is A reel, B is B reel, ... F is F reel)

2^{nd} digit: Winding Machine No. (“9” is No. 9 winder)

Spec. No.	INR18650-20R	Version No.	1.2	In-Young Jang

Revision history

Version	Date('yr-m-d)	Changes/Author	Reason of change
1.0	'11-12-05	In-Young Jang	First version
1.1	'12-01-04	In-Young Jang	Lot marking
1.2	'12-05-18	OCV change: 3.600~3.690V / In-Young Jang	Typo correction of shipping OCV
		Max. continuous discharge : 22A /In-Young Jang	Optimized Max. continuous discharge current